INFORMATION TO USERS

This manuscript has been reproduced from the microfilm master. UMI films the text directly from the original or copy submitted. Thus, some thesis and dissertation copies are in typewriter face, while others may be from any type of computer printer.

The quality of this reproduction is dependent upon the quality of the copy submitted. Broken or indistinct print, colored or poor quality illustrations and photographs, print bleedthrough, substandard margins, and improper alignment can adversely affect reproduction.

In the unlikely event that the author did not send UMI a complete manuscript and there are missing pages, these will be noted. Also, if unauthorized copyright material had to be removed, a note will indicate the deletion.

Oversize materials (e.g., maps, drawings, charts) are reproduced by sectioning the original, beginning at the upper left-hand corner and continuing from left to right in equal sections with small overlaps.

ProQuest Information and Learning
300 North Zeeb Road, Ann Arbor, MI 48106-1346 USA
800-521-0600

Université d'Ottawa · University of Ottawa

National Library of Canada
Acquisitions and Bibliographic Services
395 Wellington Street
Ottawa ON K1A 0N4
Canada

Bibliothèque nationale du Canada
Acquisitions et services bibliographiques
395, rue Wellington
Ottawa ON K1A 0N4
Canada

Your file Votre référence

Our file Notre référence

The author has granted a non-exclusive licence allowing the National Library of Canada to reproduce, loan, distribute or sell copies of this thesis in microform, paper or electronic formats.

The author retains ownership of the copyright in this thesis. Neither the thesis nor substantial extracts from it may be printed or otherwise reproduced without the author's permission.

L'auteur a accordé une licence non exclusive permettant à la Bibliothèque nationale du Canada de reproduire, prêter, distribuer ou vendre des copies de cette thèse sous la forme de microfiche/film, de reproduction sur papier ou sur format électronique.

L'auteur conserve la propriété du droit d'auteur qui protège cette thèse. Ni la thèse ni des extraits substantiels de celle-ci ne doivent être imprimés ou autrement reproduits sans son autorisation.

0-612-76631-4

Canada

Abstract

Two separate case studies on polymerization kinetics were performed. These studies focused on the determination of reactivity ratios: important copolymerization kinetic parameters. They are used to predict multicomponent polymer composition directly and have an indirect influence on the prediction of polymerization rate and final properties. In some cases, these parameters can be very difficult to obtain using standard techniques. These standard methods involve low conversion experiments and measurement of the final polymer composition.

The goal of the first study was to determine the reactivity ratios of a copolymer system that presents significant experimental challenges. The study involved a small polymer chain, called a macromonomer copolymerized with acrylic or methacrylic acid monomers. Due to the presence of the acid monomers, extremely high reaction rates made the experiments difficult to control. In addition, the macromonomer was very difficult to separate from the polymer due to their molecular similarities. Furthermore, measurement of copolymer composition using standard techniques such as ^{1}H-NMR spectrometry was impossible. These issues were resolved using Gel Permeation Chromatography (GPC), but the results obtained were inconclusive.

The second case study involved the styrene/butyl acrylate copolymer system. Firstly, the reactivity ratios were estimated in bulk and in toluene solution. The solvent was found to have an insignificant effect on the reactivity ratios and prediction of polymer composition. Further investigation of the styrene/butyl acrylate solution copolymerization to high conversion levels was initiated. It was observed that the rate of polymerization decreased with increasing amounts of styrene in the feed. In addition, when the composition of styrene was near the azeotropic composition, composition drift was not significant.

Gel permeation chromatography (GPC) was used to determine the weight-average molecular weight of selected styrene/butyl acrylate copolymer samples. Relatively low molecular weight polymer was generated and this was attributed to the chain transfer and dilution effects of the solvent as well as the chain transfer effect of a chain transfer agent.

An additional investigation focused on the use of attenuated total reflectance-Fourier transform infrared (ATR-FTIR) spectrometry was completed. The ATR-FTIR data were obtained using the ReactIR 1000 reaction analysis system and were compared to traditional techniques to determine the reliability of ATR-FTIR spectrometry off-line to measure the overall conversion and individual monomer conversions. Results from the ATR-FTIR technique agreed with the gravimetric and ^{1}H-NMR spectrometry data for most of the reaction conditions. However, the technique was found to underestimate the conversion when both monomer types were present in near equal amounts.

Résumé

Deux cas séparés sur la cinétique de polymérisation ont été réalisés. Cette étude visait la détermination des rapports de réactivité. Les rapports de réactivités sont des paramètres importants pour la caractérisation des copolymères. Les rapports de réactivité sont utilisés pour prédire la composition d'un polymère à plusieurs composants ainsi que les propriétés finales du polymère. Dans certains cas, ces paramètres peuvent être difficiles à obtenir en utilisant des techniques normales. Pour déterminer les rapports de réactivité, des expériences à basse conversion doivent être exécutées et la composition de l'alimentation et du polymère final doit être mesurée.

Le but du premier système est de déterminer le rapport de réactivité d'un copolymère qui présente un défi très grand au niveau expérimental. Ce système implique l'utilisation d'une courte chaîne de polymère, appelée macromonomère, copolymérisé avec un monomère d'acide acrylique ou d'acide méthacrylique. En raison de la présence des monomères d'acide, les taux de réactions obtenues sont extrêmement élevés ce qui rend les réactions difficiles à contrôler. De plus, le macromonomère a été très difficile à séparer du polymère en raison de leur similarité moléculaire. De plus, la mesure de la composition du copolymère en utilisant des techniques standard comme la spectrométrie ^{1}H-RMN était impossible. Ces problèmes ont été résolus grâce à l'utilisation de la chromatographie par exclusion. Cependant, les résultats obtenus étaient non-concluants.

L'autre système étudié était celui relié au système styrène/acrylate de butyle. Premièrement, les rapports de réactivité ont été estimés en polymérisation de masse puis en solution avec du toluène. Le solvant avait une influence non-signifiante sur les résultats des rapports de réactivité ainsi que sur la prédiction de la composition du polymère final. Une étude plus poussée sur la copolymérisation en solution pour le système styrène / acrylate de butyle à haute conversion a été exécutée. Les observations suivantes ont été remarqués : Le taux de polymérisation diminuait lorsque la quantité de styrène dans l'alimentation augmentait. Aussi, lorsque la composition du styrène s'approchait de la composition azéotropique, la dérive de composition devenait non-significative.

La chromatographie par exclusion (GPC) a été utilisée pour déterminer le poids moléculaire moyen de certains échantillons de copolymères. De façon générale, les poids moléculaires moyens sont faibles, ceci est dû aux transferts de chaînes ainsi qu'aux effets de dilution du solvant.

Une étude supplémentaire centrée l'utilisation du facteur de réflexion total atténué – spectroscopie infrarouge de la transformation de Fourier (ATR-FTIR). Les résultats du ATR-FTIR ont été obtenus via le système d'analyseur ReactIR 1000. Ces résultats ont été comparés avec les techniques traditionnelles afin de déterminer la fiabilité du spectromètre pour évaluer la conversion totale et individuelle. Les résultats obtenus ont été comparés avec les résultats provenant de la gravimétrie et du spectromètre ^{1}H-RMN pour la chaque condition de réaction. Généralement, l'infrarouge tend à sous-estimer la conversion lorsque les monomères de chaque type sont présentes en quantités égales dans l'échantillon.

Acknowledgements

I want to express my gratitude to my supervisor, Dr. Marc A. Dubé. Thanks Marc for your great patience, support, and guidance throughout this work. Thanks also to the technicians Louis Tremblay, Gérard Nina and Franco Ziroldo for the help they provided during this work. Many thanks to all my friends I had throughout these years: Malik Hakim, Chris Badeen, Hong Hua and Renata Jovanovic. We had nice time together making polymer and sharing computers. Grateful thanks go to my parents, Gaston and Marie-Paule, they are so far away but so close in my life. Also, thanks to my parents-in-law, Réal and Lorraine for your support. Finally, I would like to thank my fiancée, Karina, for your constant help even during the toughest moments.

To Karina...

Table of Contents

List of Figures

List of Tables

Nomenclature

Symbols

Abs = Absorbance

f = Initiator efficiency

f_i = mole fraction of monomer i

f_{i0} = Initial mole fraction of monomer i

f_{i0}' = Monomer mole fraction in the feed for reactivity ratio estimation

f_{i0}'' = Monomer mole fraction in the feed for reactivity ratio estimation

F_i = Instantaneous mole fraction of monomer i

I = Initiator

[I] = Initiator concentration

k_d = Initiator decomposition rate constant

k_{fP} = Chain transfer to polymer rate constant

k_{fT} = Chain transfer to small molecule rate constant

k_i = Initiation rate constant

k_p = Propagation rate constant

k_p^* = Terminal and internal double bond reaction rate constant

k_{pmn} = Rate of a propagating radical chain ending in monomer m adding monomer n

k_t = Termination rate constant

k_{tc} = Termination by combination rate constant

k_{td} = Termination by disproportionation rate constant

K' = Mark-Houwink coefficient

M_j = Monomer j

M_j^* = Monomer radical j

$[M_j]$ = Concentration of monomer j

$[M_j^*]$ = Concentration of monomer radical j

$M_{m,n}$ = Monomer of chain length m ending in monomer n

$M_{m,n}^*$ = Monomer radical of chain length m ending in monomer n

M_W = Weight-average molecular weight

MW_i = Molecular Weight of monomer i

r_i = Reactivity ratio of monomer i

R_I = Rate of initiation

$R_I^{\bullet}$ = Initiator radical

S = Small molecule

$S^{\bullet}$ = Small molecule with a radical

T = Temperature

x = Molar monomer conversion

x_i' = Individual molar monomer conversion

X = Overall mass monomer conversion

Greek Letters

α = Meyer-Lowry parameter

α' = Mark-Houwink coefficient

β = Meyer-Lowry parameter

δ = Meyer-Lowry parameter

γ = Meyer-Lowry parameter

List of Abbreviations

AA = Acrylic Acid

AIBN = 2,2'- Azobisisobutyronitrile

ATR-FTIR spectrometry = Attenuated Total Reflectance Infrared Spectrometry

BA = Butyl Acrylate

^{13}C-NMR Spectrometry = Carbon 13 Nuclear Magnetic Resonance Spectrometry

CTA = Chain Transfer Agent

EVM = Error-in-Variables Model

GPC = Gel Permeation Chromatography

^{1}H-NMR Spectrometry = Proton Nuclear Magnetic Resonance Spectrometry

MAA = Methacrylic Acid

MMA = Methyl Methacrylate

Mv = Millivolts

MW = Molecular Weight

NaOH = Sodium Hydroxide

P(AA) = Polyacrylic Acid

PEO = Polyethylene Oxide

P(MAA) = Polymethacrylic Acid

ppm = Parts per Million

RREVM = Reactivity Ratio using Error-in-Variables Model

Sty = Styrene

THF = Tetrahydrofuran

Vac = Vinyl Acetate

vol. % = Volume Percent

wt. % = Weight Percent

Structure of the chemicals

2,2-Azobisisobutyronitrile (AIBN)

Molecular Weight = 164.2096 g / mol

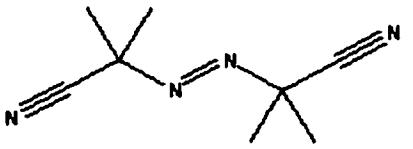

Di-tert-butyl-peroxide (Trigonox B)

Molecular Weight = 146.229 g / mol

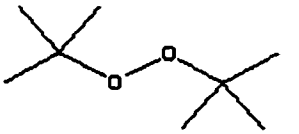

Acrylic Acid

Molecular Weight = 72.0634 g / mol

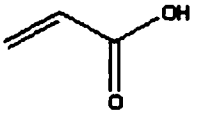

Methacrylic Acid

Molecular Weight = 86.0902 g / mol

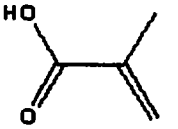

Butyl Acrylate

Molecular Weight = 128.1706 g / mol

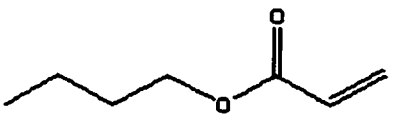

Styrene

Molecular Weight = 104.1512 g / mol

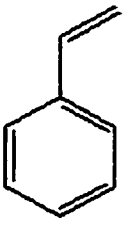

Chapter 1

Introduction

Polymers are long chain molecules or macromolecules composed of small repeat units or monomers. Due to their size, polymers offer many unique properties that have allowed their use in a wide variety of applications such as tubing, paints, computer parts, etc. Often, in an effort to combine a variety of properties, three or more different monomers can be reacted in a multicomponent system. In this case, important parameters known as reactivity ratios are needed. Reactivity ratios describe the affinity of a free radical to react with one monomer compared to another. Reactivity ratios are used to predict copolymer composition, which directly affects the final properties of the polymer. In addition, reactivity ratios affect the rate of polymerization, which, in turn, affects the molecular weight distribution and ultimately the final properties of the polymer.

Several methods exist for the estimation of reactivity ratios. Typically, homogenous or bulk polymerization experiments are run to low conversion levels (< 5 wt. % conversion) after which the polymerization is halted and the polymer is separated from the monomer by precipitating the polymer in a non-solvent which is solvent for the monomer (e.g. ethanol). The polymer is then separated from the solvent mixture, dried and analyzed for its composition using a technique such as ^{1}H-NMR spectrometry. Then, the feed composition and the final polymer composition are input to a non-linear parameter estimation program to estimate the reactivity ratios. In some cases, the estimation of reactivity ratios can be experimentally challenging. For example, separation

of the polymer from the monomer after polymerization may be impossible using standard techniques. Furthermore, the polymer composition may be difficult to measure due to the overlap of the peaks in the ^{1}H-NMR spectra or due to the insolubility of the polymer in common solvents.

In this thesis, two case studies have been investigated.

The first case study is considered to be challenging for the purposes of reactivity ratio measurement. The system involves the copolymerization of a macromonomer with a carboxylic acid monomer. The polymers from these systems are very difficult to separate from the macromonomers with a simple precipitation due to the high viscosity of the system and the similar nature of the macromonomer to the polymer (i.e. macromonomer has an appreciable molecular weight). In addition, the analysis of this polymer is complicated by the fact that the comonomers have overlapping peaks in the ^{1}H-NMR spectrum. Furthermore, the achievement of low conversion is difficult due to the highly reactive nature of carboxylic acid monomers. The objective of this first case study was to get efforts to overcome difficulties in order to estimate the reactivity ratios of this copolymer system.

The second case study involved the styrene/butyl acrylate copolymerization in bulk and in toluene solution. The main objective was to evaluate the extent of any solvent on the polymerization kinetics. Both low and high solution copolymerization were performed. A secondary objective was to continue an ongoing evaluation of ATR-FTIR spectrometry to monitor conversion and polymer composition.

1.1 Thesis Outline

This thesis comprises seven chapters supplemented by a reference section as well as an appendix that contains all of the experimental results and sample calculations.

Chapter 2 contains a survey of the literature and is divided in two sections. The first section concerns the copolymerization of a carboxylic acid monomer with a macromonomer. The next section concerns the Styrene/Butyl Acrylate system.

Chapter 3 discusses multicomponent polymerization kinetic theory.

In Chapter 4, descriptions of the experimental procedures and characterization methods used in this thesis are given. The procedures include monomer purification, monomer distillation, polymerization, and macromonomer separation from the polymer. Due to the nature of this thesis, this chapter is of major importance. Novel experimental techniques as well as modifications to existing ones are discussed.

In Chapter 5, the macromonomer/carboxylic acid monomer systems are discussed with a focus on reactivity ratio estimation.

Chapter 6 contains results from the bulk and solution polymerization of styrene/butyl acrylate. Solvent effects on the polymerization kinetics are discussed. An ATR-FTIR technique is compared to results obtained using gravimetry and ^{1}H-NMR spectroscopy. Also, a model used to predict polymerization kinetics is compared to experimental data.

Conclusions and recommendations are presented in Chapter 7.

Chapter 2

Literature Survey

2.1 Carboxylic Acid Monomer/Macromonomer System

This system was studied for the purpose of contract research and thus, I am bound by a confidentiality agreement to not reveal the exact identity of the macromonomer. There are only a few reported studies of the copolymerization of carboxylic acid monomers and macromonomers.

Jeon et al. (1988) examined the p(AA)/PEO and the p(MAA)/PEO complex formation in solid state through hydrogen bonding. This investigation was done with differential scanning calorimetry (DSC) and Fourier-transform infrared (FT-IR) spectroscopy. They reported the melting temperature and the degree of crystallinity of the blended systems. They also explained solvent effects and hydrophobic effects on the complexation.

In the open literature, there are no reports of bulk copolymerization of macromonomer with an acid monomer. This is not surprising due to the relative novelty and confidentiality surrounding these systems.

2.2 Sty/BA Copolymerization

Several publications discuss Sty/BA copolymerization. While many of these deal with emulsion polymerization, relevant to this thesis are those covering bulk and solution copolymerization.

2.2.1 Bulk Copolymerization of Styrene/Butyl Acrylate

The Sty/BA system has many industrial applications: it is used in paints, coatings and adhesives. This copolymer system has not been studied extensively as a bulk polymerization but has been studied in some detail as an emulsion polymerization. Some of the few kinetic studies of the bulk copolymerization are discussed below.

Dubé et al. (1990), examined the bulk copolymerization of BA/Sty at 50°C with 2,2'-Azobisisobutyronitrile (AIBN) initiator. A series of low conversion experiments (<7%) designed using the Tidwell-Mortimer criterion (Tidwell and Mortimer, 1965) were run. Copolymer composition analysis was performed using ^{1}H-NMR spectroscopy. The reactivity ratios were determined using an error-in-variables model methods (EVM) (Dubé et al., 1991). Full conversion experiments were also run at two different initiator concentrations and different monomer feed compositions. Data for conversion, copolymer composition and number- and weight-average molecular weights were also reported.

Kostański et al. (1991), studied the bulk copolymerization of Sty/BA at high temperatures (110°C, 150°C and 170°C) with no initiator. They determined the copolymer composition with IR spectroscopy. Reactivity ratios were determined using two methods: the Kelen-Tüdös method (Kelen and Tüdös, 1975) and EVM method (Patino-Leal et al., 1980). These methods yielded similar results.

Brar et al. (1992) analyzed the bulk copolymerization of Sty/BA at 70°C using 0.5% weight by volume of benzoyl peroxide initiator. The conversion levels were maintained between 5% and10 %. The system was analyzed for copolymer composition using ^{1}H-NMR spectra and the monomer reactivity ratios were calculated using a

nonlinear least squares EVM method. ^{13}C-NMR spectra for the Sty/BA system were also presented.

Lahoud (1998) presented two sets of reactivity ratios estimation from a bulk copolymerization at 50°C using AIBN as initiator. The conversion was held at levels less than 3%. An EVM program developed by Dubé et al. (1991) and later updated by Polic et al. (1995) was employed to determine the reactivity ratio estimates using data acquired through ^{1}H-NMR.

Reactivity ratio estimates for this system are summarized in Table 2.1.

Table 2.1: Literature review on the Styrene/Butyl Acrylate system

Authors	Year	Type	Solvent	T(°C)	r_{Sty}	r_{BA}
Arlman and Melville	1950	Solution	-	25	0.48	0.15
Bradbury and Melville	1954	Solution	-	60	0.76	0.15
Gruber and Knell	1978	Solution	-	70	0.63	0.20
Hamaide et al.	1984	Solution	-	60	0.94	0.22
Dubé et al.	1990	Bulk		50	0.955	0.183
Kostanski and Hamielec	1991	Bulk		110	0.79	0.25
recalculated EVM	-	-		-	0.80	0.25
Kostanski and Hamielec	1991	Bulk		150	0.79	0.34
recalculated EVM	-	-		-	0.78	0.34
Kostanski and Hamielec	1991	Bulk		170	0.75	0.38
recalculated EVM	-	-		-	0.76	0.38
Brar and Satyanarayana	1992	Bulk		70	1.21	0.17
Ziaee and Nekoomanesh	1998	Solution	Toluene	80	0.883	0.207
Lahoud	1998	Bulk		50	0.5228	0.188
Lahoud	1998	Bulk		50	0.5623	0.2329
Fernandez-Garcia et al.	2000	Bulk		50	0.865	0.189
Fernandez-Garcia et al.	2000	Solution	Benzene	50	0.842	0.176
Fernandez-Garcia et al.	2000	Solution	Benzonitrile	50	0.734	0.330

2.2.2 Solution Copolymerization of Styrene/Butyl Acrylate

Solution polymerizations of the Sty/BA system are discussed in some of the papers listed in Table 2.1. From the point of view of solution polymerization and solvent effect relative to this system, some key papers were reported in more detail below.

Ziaee and Nekoomanesh (1998) studied the Sty/BA copolymerization using toluene as a solvent and benzoyl peroxide as initiator. Runs were performed at low and high conversion at a temperature of 80°C. They used different models for the reactivity ratio estimation and determined the conversion effect on the reactivity ratio.

Fernandez-Garcia et al. (2000) studied the benzene and the benzonitrile effects on the reactivity ratios. Bulk and solution copolymerizations of Sty/BA were performed at 50°C using AIBN as initiator. Both solvent had a significant effect on the reactivity ratios results and on the final composition of the polymer.

2.3 Mathematical Modeling and Simulation of Polymerization

Mathematical models were used to predict polymer properties during the polymerization reaction. In this thesis, a particular model has been used to predict polymer properties. The model was created by Badeen (2000) and was written in java. This model was used to estimate the reaction time for the styrene / butyl acrylate system in bulk and solution polymerization.

2.4 Polymerization Monitoring using ATR-FTIR

Many authors investigated on-line or in-line monitoring using ATR-FTIR, but few have studied off-line monitoring. In this thesis, the off-line monitoring are a very important topic. Some key articles concerning off-line monitoring using ATR-FTIR are described below.

Hua and Dubé investigated the Butyl acrylate / Methyl Methacrylate (MMA) / Vinyl Acetate (VAc) solution homo- and copolymerization using off-line monitoring via

ATR-FTIR. The monomer conversion and copolymer composition as function of time were calculated by monitoring the peak height of characteristic absorbance of monomers. The results from ATR-FTIR were comparable to those obtained by gravimetry and ^{1}H-NMR spectroscopy.

Jovanovic and Dubé (2001) studied the BA/VAc solution homopolymerization and copolymerization in toluene. Conversion and composition were monitored using ATR-FTIR spectroscopy and compared to traditional techniques (gravimetry and ^{1}H-NMR spectroscopy). Data obtained using off-line mode ATR-FTIR shows very good agreement compared with traditional techniques.

2.5 Influence of solvent on polymerization

Polymerization of monomers in a solvent overcomes many inconveniences of bulk polymerization. The solvent facilitates mixing because the viscosity is greatly decreased. It acts as a diluent and helps transfer the heat of polymerization. The control of the reaction temperature is thus much easier in solution polymerization compared to bulk. However, the presence of solvent has drawbacks: chain transfer to solvent may affect molecular weight and its presence in the reaction media can affect the final purity of the polymer due to the difficulties of solvent removal from the polymer (Odian, 1991).

Different solvents can be used in solution polymerization but many have their challenges. In this thesis, toluene was used as solvent due to its good compatibility with the styrene/butyl acrylate system. Also, the toluene does not affect the characterization of the reaction mixture using the ATR-FTIR, which is a very important issue in the work.

Chapter 3

Polymerization Kinetics

The following theory is applicable for all monomers or macromonomers that add together to form a polymer.

3.1 Stages of Free Radical Polymerization

For the systems of interest in this study, polymers were produced by free-radical chain growth polymerization. This type of polymerization is accomplished by the production of free radicals (initiation step) that sequentially add monomer to create a growing polymer chain (propagation step) and eventually undergo a bimolecular termination step.

3.1.1 Initiation

During initiation, initiator radicals are produced by the homolytic dissociation of an initiator. The initiator, I, will produce a pair of initiator radicals, $R_I^{\bullet}$, as follows:

$$I \xrightarrow{k_d} 2R_I^{\bullet} \tag{3.1}$$

The initiators used in this thesis were Trigonox B (di-tert-butyl-peroxide) and AIBN (2,2'-Azobisisobutyronitrile), and were thermally activated.

Initiator radicals can recombine; this behavior is called the cage effect. This initiator behavior effectively reduces the initiator efficiency. The rate of the production of primary radicals by thermal homolysis of the initiator, which are single molecules with an electric charge, is given by:

$$R_I = 2fk_d[I] \tag{3.2}$$

where f is the initiator efficiency, k_d is the decomposition reaction rate constant and [I] is the initiator concentration.

After the initiator radicals are produced, the production of primary radicals will then occur. The primary radical is the product of the reaction between an initiator radical and a monomer, as shown by the following equation:

$$R_I^{\bullet} + M_j \xrightarrow{k_i} M_{1,j}^{\bullet} \tag{3.3}$$

In equation 3, a newly formed radical, $R^{\bullet}_I$, adds to monomer j to produce monomer radical, $M^{\bullet}_{1,j}$, with an initiation rate constant k_i. The primary radical will then add monomer via propagation.

3.1.2 Propagation

Propagation involves the sequential growth of polymer radicals through the addition of monomer molecules according to the following relation:

$$M_{n,i}^{\bullet} + M_j \xrightarrow{k_p} M_{n+1,j}^{\bullet} \tag{3.4}$$

In equation 4, monomer M_j, adds to a radical of chain length n, ending in monomer i, $M^{\bullet}_{n,i}$, to form a radical of chain length n+1 ending in monomer j, $M^{\bullet}_{n+1,j}$, with a propagation rate constant, k_p.

This polymerization reaction occurs very quickly so that typically, a chain of a thousand units long can be formed within a second.

3.1.3 Termination

Termination is the bimolecular annihilation of free radicals, which results in the stoppage of polymer chain growth. Termination can occur by combination or by disproportionation.

Termination by combination occurs when two radical chains, called $M^{\bullet}_{n,i}$ and $M^{\bullet}_{m,j}$, diffuse close to each other to form one larger "dead" polymer chain of length m+n, M_{m+n}, with a termination by combination rate parameter, k_{tc}. This termination behavior is represented by the following equation:

$$M^{\bullet}_{n,i} + M^{\bullet}_{m,j} \xrightarrow{k_{tc}} M_{m+n} \tag{3.5}$$

Termination by disproportionation occurs when two radical-ended molecules called $M^{\bullet}_{n,i}$ and $M^{\bullet}_{m,j}$, mutually terminate their respective free radicals which leads to the formation of two "dead" polymer chains of length m and n, M_m and M_n, with a termination by disproportionation rate parameter, k_{td}. This behavior is represented by the following relationship:

$$M^{\bullet}_{n,i} + M^{\bullet}_{m,j} \xrightarrow{k_{td}} M_m + M_n \tag{3.6}$$

In each of those two cases, $M^{\bullet}_{n,i}$, represents a radical chain of length n ending in monomer i whereas $M^{\bullet}_{m,j}$ has a chain length m and ends in monomer j. The M_m, M_n or M_{m+n} represent a dead polymer chain of length m, n or m+n, respectively.

The total rate parameter for termination is then expressed by the addition of the rate parameters for combination and disproportionation:

$$k_t = k_{tc} + k_{td} \tag{3.7}$$

Often, the rate of termination is diffusion-controlled and k_t does not remain constant but rather, decreases rapidly with increasing viscosity of the reaction mixture.

3.2 Chain Transfer theory

3.2.1 Chain Transfer to small molecules (S)

At any point during the propagation reaction, the growing radical may transfer its active center to a small molecule (S), such as monomer, initiator, solvent, impurity or chain transfer agent (CTA). This mechanism is shown as follows:

$$M_{n,i}^{\bullet} + S \xrightarrow{k_{fT}} M_{n,i} + S^{\bullet} \tag{3.8}$$

Such a reaction prematurely terminates a growing chain. In equation 8, the polymer radical of chain length n ending in monomer i, $M^{\bullet}_{n,i}$, transfers its radical to a small molecule S resulting in a dead polymer chain of length n ending in monomer i, $M_{n,i}$. The transferred radical usually continues to react. This results in a negligible effect on the reaction rate and an appreciable reduction in polymer molecular weight.

3.2.2 Chain Transfer to polymer

In a mechanism similar to that of chain transfer to small molecules, the active center may transfer to a dead polymer chain, creating branched instead of linear polymer. The reaction progresses as follows:

$$M_{n,i}^{\bullet} + M_{m,j} \xrightarrow{k_{fP}} M_{n,i} + M_{m,j}^{\bullet} \tag{3.9}$$

Such a reaction involves a polymer radical chain of length n ending in monomer i, $M^{\bullet}_{n,i}$, that transfers its radical to a dead polymer chain of length m ending in monomer j, $M_{m,j}$. This yields a dead polymer chain of length n ending in monomer i, $M_{n,i}$, and a polymer radical of length m ending in monomer j, $M^{\bullet}_{m,j}$.

3.2.3 Terminal and internal double bond reactions

The reaction of the active center with a terminal or internal double bond on the dead polymer chain is another cause of long chain branching. The reaction is as follows:

$$M^{\bullet}_{n,i} + M_{m,j} \xrightarrow{k^{\bullet}_{p}} M^{\bullet}_{n+m,i+j} \tag{3.10}$$

Such a reaction involves a polymer radical chain of length n ending in monomer i, $M^{\bullet}_{n,i}$, that will attach to a dead polymer chain of length m ending in monomer j, $M_{m,j}$. The results of this reaction will be a bigger polymer radical chain of length n+m.

3.3 Copolymer composition theory

When two different monomers combine, they form a copolymer. This copolymer will have the combined properties from both polymers. Monomers combine to form copolymer in the following manner:

$$M^{\bullet}_{1} + M_{1} \xrightarrow{k_{p11}} M^{\bullet}_{1} \tag{3.11}$$

$$M^{\bullet}_{1} + M_{2} \xrightarrow{k_{p12}} M^{\bullet}_{2} \tag{3.12}$$

$$M^{\bullet}_{2} + M_{1} \xrightarrow{k_{p21}} M^{\bullet}_{1} \tag{3.13}$$

$$M^{\bullet}_{2} + M_{2} \xrightarrow{k_{p22}} M^{\bullet}_{2} \tag{3.14}$$

where k_{p11} is the rate parameter for a propagating radical chain ending in monomer 1 adding monomer 1, k_{p12} is that for a propagating radical chain ending in monomer 1 adding monomer 2, and so on. This mechanism is referred to as the terminal or Mayo-Lewis model which implies that the kinetics of the propagation step are dictated only by the last monomer to add to the end of the polymer chain.

3.3.1 Mayo-Lewis Equation

From the polymerization mechanism shown above, the rates of disappearance of each monomer, which are exactly the same as the rate of addition of monomer into the copolymer (Mayo-Lewis, 1944), are given as follows:

$$-\frac{d[M_1]}{dt} = k_{p11}[M_1^\bullet][M_1] + k_{p21}[M_2^\bullet][M_1] \tag{3.15}$$

$$-\frac{d[M_2]}{dt} = k_{p12}[M_1^\bullet][M_2] + k_{p22}[M_2^\bullet][M_2] \tag{3.16}$$

The ratio of equation 15 over 16 gives the copolymer composition as:

$$\frac{d[M_1]}{d[M_2]} = \frac{k_{p11}[M_1^\bullet][M_1] + k_{p21}[M_2^\bullet][M_1]}{k_{p12}[M_1^\bullet][M_2] + k_{p22}[M_2^\bullet][M_2]} \tag{3.17}$$

Equation 17 is commonly simplified and re-arranged into the following form known as the Mayo-Lewis equation:

$$\frac{F_1}{F_2} = \frac{(r_1 f_1 + f_2) f_1}{(f_1 + r_2 f_2) f_2} \tag{3.18}$$

where two reactivity ratios are defined as:

$$r_1 = \frac{k_{p11}}{k_{p12}} \tag{3.19}$$

$$r_2 = \frac{k_{p22}}{k_{p21}} \tag{3.20}$$

F_1 and F_2 are the instantaneous mole fractions of monomer 1 and monomer 2 in the copolymer, respectively, and f_i is the mole fraction of monomer i in the mixture. The parameters r_1 and r_2, the monomer reactivity ratios, are the ratios of the rate constants for a reactive propagating species adding its own type of monomer to the rate constant for the addition of the other monomer. From the Mayo-Lewis equation, it is evident that the reactivity ratios are crucial for the prediction of polymer composition and hence, the microstructure, polymerization rate and ultimately the molecular weight distribution. All of these directly influence the final product properties.

The Mayo-Lewis equation can be used for the estimation of reactivity ratios only in situations where composition drift is negligible. This typically occurs at conversion levels lower than 10 wt.%. However, composition drift is highly dependent on the value of the reactivity ratios (Dubé and Penlidis, 1995).

3.3.2 Meyer-Lowry Equation

For situations when composition drift is significant, the integrated version of the Mayo-Lewis equation, the Meyer-Lowry integrated copolymer equation (Meyer and Lowry, 1965), is used:

$$x = 1 - \left(\frac{f_1}{f_{10}}\right)^{\alpha} \left(\frac{1-f_1}{1-f_{10}}\right)^{\beta} \left(\frac{f_{10}-\delta}{f_1-\delta}\right)^{\gamma} \tag{3.21}$$

where x is the molar monomer conversion, f_{10} is the initial mole fraction of monomer 1, f_1 is the mole fraction of monomer 1 and:

$$\alpha = \frac{r_2}{1-r_2} \qquad (3.22)$$

$$\beta = \frac{r_1}{1-r_1} \qquad (3.23)$$

$$\delta = \frac{1-r_2}{2-r_1-r_2} \qquad (3.24)$$

$$\gamma = \frac{1-r_1 r_2}{(1-r_1)(1-r_2)} \qquad (3.25)$$

The full conversion range integrated Meyer-Lowry expression excludes the requirements of a negligible composition drift assumption.

3.4 Reactivity Ratio Estimation

When attempting to predict product quality and production rates for multicomponent polymerizations, the accuracy of the reactivity ratios has a significant impact on model predictions. Poor model predictions can often be mistakenly attributed to a poor model when the cause is actually inaccuracy in the reactivity ratios. Several approaches to measuring reactivity ratios have been proposed over the years but several statistically incorrect estimation methods continue to persist (Polic et al., 1998). The method that has been shown to be the most reliable is that employing the error-in-variables model (EVM) (O'Driscoll and Reilly, 1987; Dubé et al., 1991; Rossignoli and Duever, 1995; Dubé et al., 1997; Polic et al., 1998). Dubé et al., 1991 developed a commercial program, known as RREVM program is restricted to the Mayo-Lewis model for copolymerizations in which composition drift is not significant; that is, at low conversion (<10 wt.%). When composition drift is significant (e.g., at high conversion levels), the Meyer-Lowry model, which is essentially the integrated form of the Mayo-

Lewis equation, is used with a non-linear parameter estimation technique (Meyer and Lowry, 1965; Dubé et al., 1991, Dubé et al., 1997).

The Mayo-Lewis model (and thus, the RREVM program) necessitates the assumption of negligible drift in copolymer composition. This factor is typically addressed in the experimental design wherein the experiments are halted at low monomer conversion levels (<10 wt.%). The selection of the initial monomer feed concentrations is performed using the Tidwell-Mortimer criterion (Tidwell and Mortimer, 1965).

$$\frac{F_1}{F_2} = \frac{\left(r_1[M_1]+[M_2]\right)[M_1]}{\left([M_1]+r_2[M_2]\right)[M_2]} \tag{3.26}$$

$$f'_{10} = \frac{2}{2+r_1} \tag{3.27}$$

$$f''_{10} = \frac{r_2}{2+r_2} \tag{3.28}$$

The Tidwell-Mortimer criterion is based on the sensitivity of the reactivity ratios to the errors encountered in the determination of the copolymer composition. Tidwell and Mortimer (1965) recommend performing several replicates at two different monomer feed compositions, f_{10}' and f_{10}'' as shown in equation 3.27 and 3.28. Preliminary estimates of the reactivity ratios are required. Such estimates may be obtained from the literature, in books such as the Polymer Handbook (1989) or from a set of preliminary experiments. The values of r_1 and r_2 are the initial reactivity ratio guesses. $[M_1]$ and $[M_2]$ are the feed composition of monomer 1 and monomer 2, respectively.

Chapter 4

Experimental Procedures

4.1 List of reagents

Monomers are typically inhibited with a free-radical scavenger to prevent polymerization from occurring during shipping or storage. The monomers and their inhibitors used in our experiments are listed below:

- Butyl Acrylate (BA, Aldrich) inhibited with 40-80 ppm methyl ethyl hydroquinone
- Styrene (Sty, Aldrich) inhibited with 10-15 ppm 4-tert-butylcatechol
- Methacrylic Acid (MAA, Aldrich) inhibited with 100-250 ppm hydroquinone
- Acrylic Acid (AA, Aldrich) inhibited with 200 ppm hydroquinone
- Macromonomer 1 (confidential) inhibited with 2000 ppm BHT and 2 ppm benzoquinone
- Macromonomer 2 (confidential) inhibited with 925 ppm BHT and 150 ppm benzoquinone

The solvents used for the experiments were used as packaged and are listed below:

- Toluene (Reagent Grade, ACP Chemicals Inc.)
- Tetrahydrofuran (THF, HPLC Grade, ACP Chemicals Inc.)
- Acetone (Reagent Grade, ACP Chemicals Inc.)
- Ethanol (denatured, ACP Chemicals Inc.)

- Cyclohexane (Reagent Grade, ACP Chemicals Inc.)
- Hexanes (Reagent Grade, ACP Chemicals Inc.)
- Diethyl Ether (Reagent Grade, BDH)

Other ingredients are listed below:

- 2,2'-Azobisisobutyronitrile (AIBN, Aldrich Chemical Company, initiator)
- Di-tert-butyl peroxide (Trigonox B, Akzo Nobel Chemicals Inc., initiator)
- N-Dodecyl Mercaptan (Sigma-Aldrich, Chain Transfer Agent)
- Sodium Hydroxide pellets (lab grade, ACP Chemical Inc.)
- Calcium Chloride Anhydrous (4-20 mesh, lab grade, ACP Chemicals Inc.)
- Potassium Hydroxide pellets (lab grade, ACS, Fisher Scientific)
- Hydroquinone (lab grade, J.T. Baker Chemical Co.)

4.2 Reagent Preparation

4.2.1 Initiator Preparation

The initiators used in these experiments were 2,2'-azobisisobutyronitrile (AIBN) and di-tert-butyl-peroxide (Trigonox B). Trigonox B was used without further purification, but AIBN was purified as described below.

A 250 mL beaker was filled with 150 mL of distilled methanol. The beaker was then immersed in a heated water bath (50°C) until it reached 40°C. AIBN was then added to the methanol until a saturated solution was produced. Next, the beaker was covered with a watch glass and placed in a freezer at -10°C for 20 minutes to recrystalize the

AIBN. The crystalline solution was filtered using a Buchner funnel. The filtered crystals were placed in the 250 mL beaker with 150 mL of distilled methanol. This procedure was repeated two times. After the creation of the third saturated solution, the beaker was left at room temperature in order to produce larger crystals. Once at room temperature, the covered beaker was placed in the freezer for 30 minutes and then filtered one last time. The purified AIBN crystals were placed in a tinted bottle covered with black tape, labeled according to WHMIS standards and stored in a freezer at -10°C. The initiator was allowed to reach room temperature before being used for the polymerization reactions.

4.2.2 Monomer preparation

A three-step procedure was employed to prepare the monomer for polymerization: inhibitor removal from the monomer, distillation of the monomer using a rotary evaporator and oxygen removal from the reaction mixture.

Inhibitor Removal

When the monomer is received from the supplier, the monomer contains a certain quantity of inhibitor. The goal of the inhibitor is to prevent it from polymerizing during shipping or storage. Therefore, the monomer was washed three times with a 10 wt.% NaOH solution in a separatory funnel to remove the inhibitor. The quantity of NaOH solution used was about one-tenth of the monomer volume. Next, the monomer was washed three times with distilled, de-ionized water in a separatory funnel using an amount of water equivalent to approximately one-tenth of the monomer volume. The "washed" monomer was then stored in a sealed Erlenmeyer flask with a small amount

(approximately one half cup) of calcium chloride at a temperature of -10°C. The calcium chloride pellets served to absorb the water present in the monomer solution after the washing operation. It is noted that the carboxylic acid monomers were exempt from the washing, because of their solubility in water. Hence, their inhibitors were removed only by distillation. For the case of the macromonomers, washes were performed using hexanes instead of 10 wt.% NaOH, and no water was used.

Monomer Distillation

In preparation for distillation, the washed monomers were removed from the freezer and allowed to reach room temperature. The monomers were distilled under vacuum using a rotary evaporator. The distillation temperatures were ≈32°C for butyl acrylate, ≈35°C for styrene and ≈40°C for methacrylic and acrylic acids, for the case of the macromonomer, the distillation step was not performed due to their high viscosity.

The first 20 ml of distilled monomer were discarded and the distillation was performed until about 20 ml of monomer were left undistilled. The distillation was performed at most 24 hours before the polymerization to minimize the formation of oligomers. After distillation, the purified solution was then stored in the freezer at -10°C.

4.2.3 Reaction Mixture Preparation

Freshly distilled monomer was removed from the freezer and allowed to reach room temperature. The reaction mixture was prepared by weighing the appropriate monomer quantities for all the ampoules. In the case of a solution polymerization, a

known quantity of toluene was added. The initiator was then added and the reaction mixture was then pipetted into glass ampoules.

Next, oxygen, a free-radical scavenger, was removed from the reaction mixture prior to polymerization. Each ampoule was connected to a degassing setup (Figure 4.1), using vacuum grease (Apeizon AP 100 high/low temperature vacuum grease) to ensure a good seal. The ampoules were then submerged in liquid nitrogen and a vacuum was applied to the contents. The valve to the manifold was then closed and the contents were allowed to thaw. Oxygen bubbles were seen to rise into the evacuated head space of the ampoules. This degassing procedure was repeated at least three times or until bubbling was no longer evident. Finally, the ampoules were flame-sealed and placed in an ice bath.

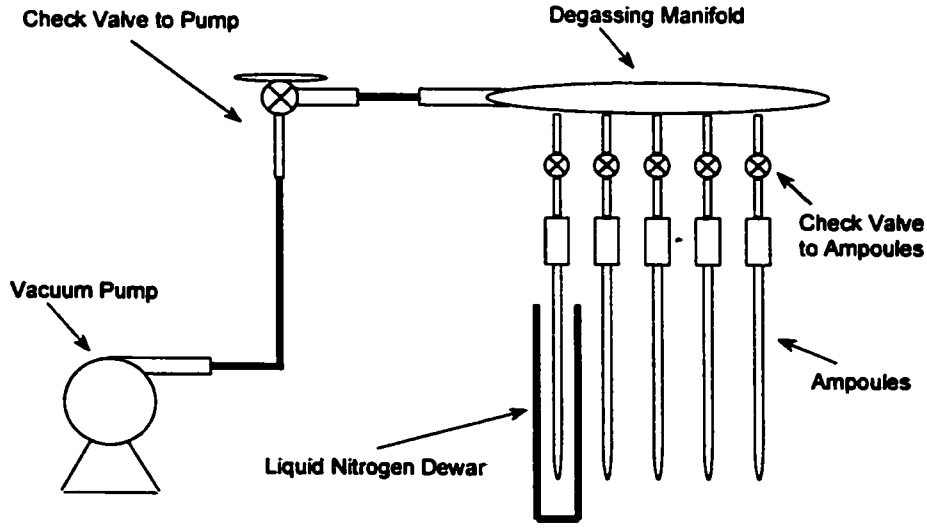

Figure 4.1: Polymerization Degassing Setup

4.3 Polymer reaction

The reactivity ratio experiments were run at low conversion levels (conversion less than 5 wt.%). This was done to minimize the effects of composition drift. The water bath was heated to the desired temperature. The ampoules were removed from the ice bath and submerged in the heated water bath for a recorded time interval. When the desired conversion level (i.e.<5wt.% by trial and error) was achieved. The ampoules were placed in ice water to quench the reaction. Each ampoule was then opened and poured into a pre-weighed dish, each broken ampoule was washed to ensure that all traces of polymer were removed. Ethanol was poured into the dish to precipitate the polymer. Samples were left in a fume-hood for about 24 hours and then placed in a vacuum oven at 40°C. After evaporation of monomer and solvents, the weight of the dried polymer and dish were recorded.

4.4 Macromonomer Case Study

I am bound by a confidentiality agreement to not reveal the identity of the macromonomers. The terms macromonomer 1 and macromonomer 2 were used throughout this thesis.

4.4.1 Method #1 for the macromonomer/acid monomer copolymer

1) Cyclohexane Wash: The contents of each ampoule were poured into a separation flask and hydroquinone was added to kill the reaction. A quantity of cyclohexane of about 50 vol.% of the ampoule contents was added to remove the unreacted acid monomer and

macromonomer. The cyclohexane wash was done three times. Then, the washed polymer mixture was poured into an Erlenmeyer flask for the neutralization step.

2) Neutralization of the acid groups: The acid groups in the polymer chains were neutralized to facilitate copolymer characterization via nuclear magnetic resonance (^{1}H-NMR spectrometry) spectrometry. To neutralize the acid groups, a solution of potassium hydroxide with a concentration of 1 mol/L was prepared. The acidity was metered using a phenolphthalein indicator that became red at a pH < 9. The target pH was reached when the colour of the solution became red. After, the neutralization step, the mixture was left sitting for a period of 24 hours in order to stabilize the neutralization reaction.

3) Liquid-liquid extraction: The liquid-liquid extraction was performed after the acid groups were neutralized. This extraction was necessary to separate the polymer from the macromonomer. The solvent used in this step was diethyl ether, and the operating temperature was about 38°C for the heater. The operating temperature was kept fairly low due to the volatility of the solvent. The liquid-liquid extraction was repeated three times with 75 ml of diethyl ether. Due to the high temperature of the polymer phase, the extractor flask was always immersed in ice before pouring the diethyl ether, this precaution prevented any flash evaporation of the diethyl ether. Each wash took at least 1 hour, in order to concentrate the solution and to remove as much macromonomer as possible. After the liquid-liquid extraction, the extract phase was stored in a freezer and the polymer phase was analyzed with ^{1}H-NMR spectrometry to determine the polymer composition.

4) NMR analysis: NMR spectrometry was used to determine the amount of each monomer chemically bound in the copolymer. Due to overlapping peaks, the use of ^{1}H-

NMR was not possible and thus, ^{13}C-NMR was employed even though quantitative results are not easily achieved with this method. This type of spectroscopy yields a measure of the extent to which electromagnetic radiation (radiant and magnetic energy) is absorbed or emitted by a sample of material. In the present case, each sample was prepared for ^{13}C-NMR using deuterium oxide as solvent. Samples that appeared to be somewhat dilute were concentrated by evaporating some of the water.

It was expected that a peak equivalent to the moles of macromonomer could be found at 175 ppm. In addition, the hydrolyzed carbonyls from the polymerized acid monomers should have been found at 183 ppm. No trace of the macromonomer was detected in the 32 samples analyzed by ^{13}C-NMR.

4.4.2 Method #2 for the macromonomer/acid monomer copolymer

1) Gel permeation chromatography (GPC) calibration: The GPC was calibrated with a variety of macromonomer/acid monomer samples. The calibration curves are shown in Figures 4.2 through 4.5.

Equations for the calibration curves for each system are as follows (b = peak area, a = amount of monomer/macromonomer in mg):

AA: $b = -6.44 \times 10^6 + 1.26 \times 10^8 a$

MAA: $b = 5.97 \times 10^7 + 9.74 \times 10^7 a$

Macromonomer 1: $b = 4.10 \times 10^6 + 2.01 \times 10^8 a$

Macromonomer 2: $b = 1.85 \times 10^7 + 1.94 \times 10^8 a$

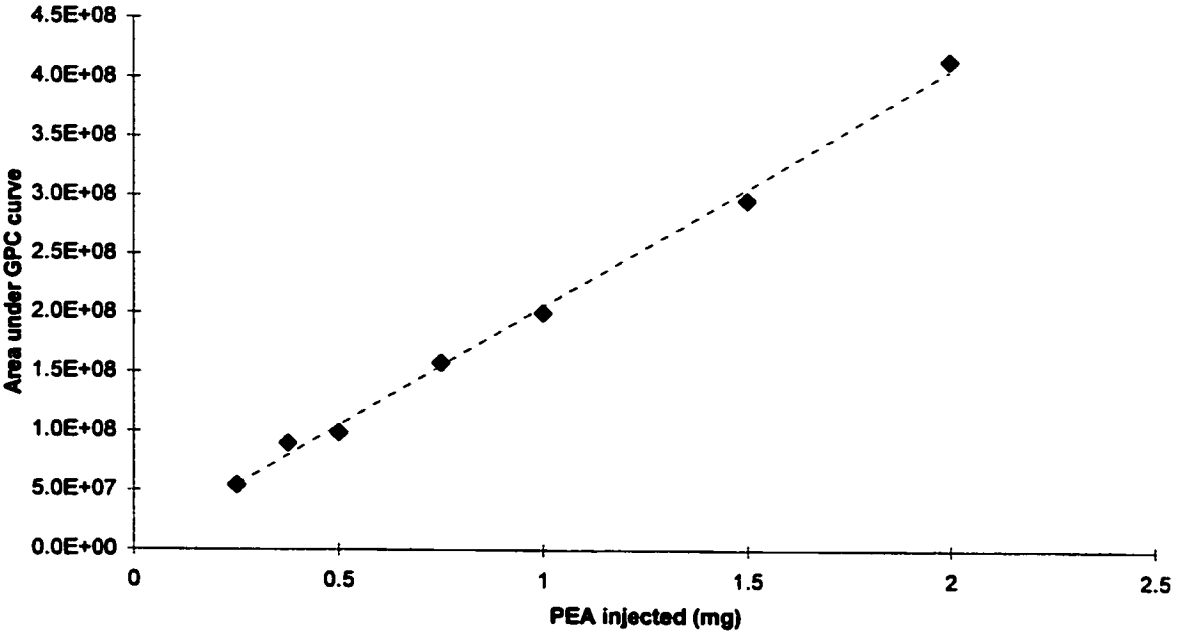

Figure 4.2: GPC Calibration Curve for Macromonomer 1

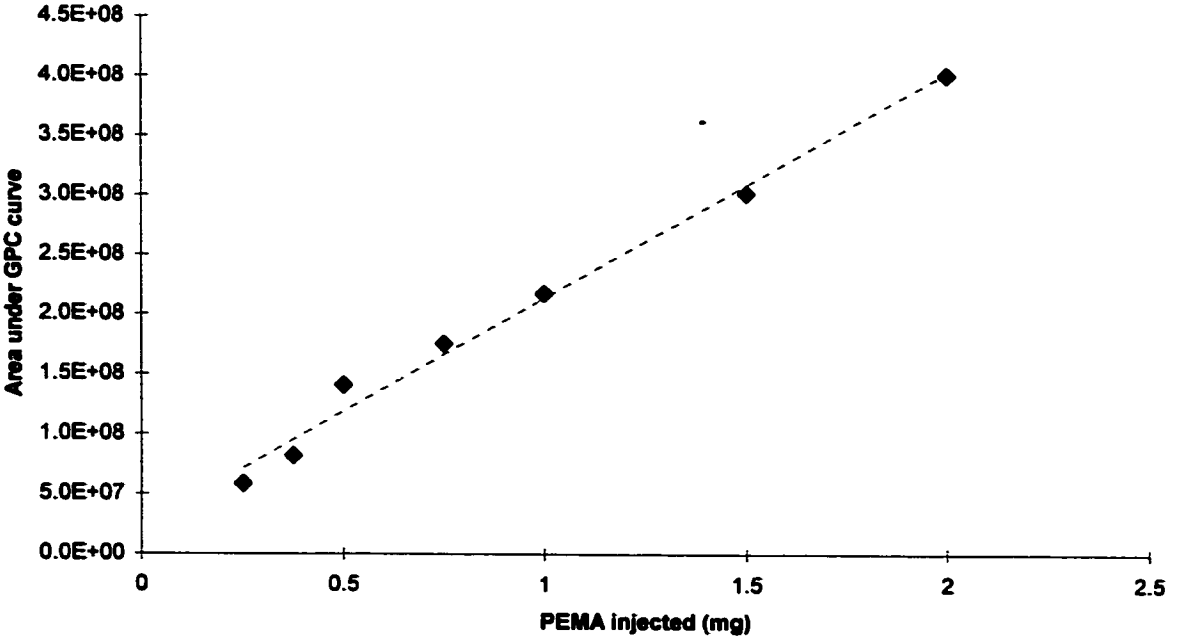

Figure 4.3: GPC Calibration Curve for Macromonomer 2

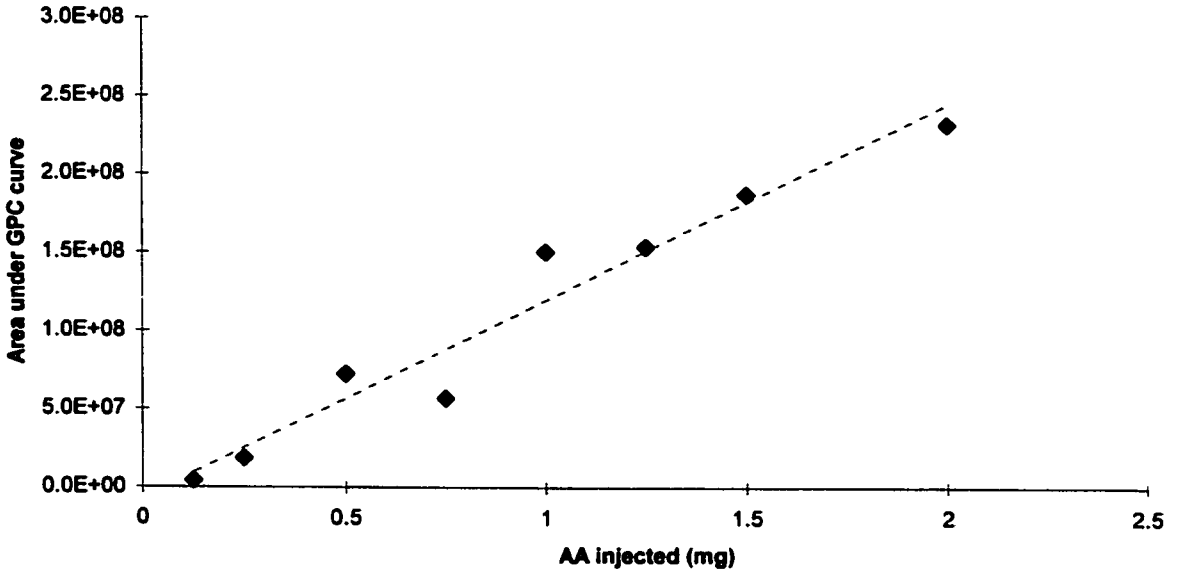

Figure 4.4: GPC Calibration Curve for Acrylic Acid

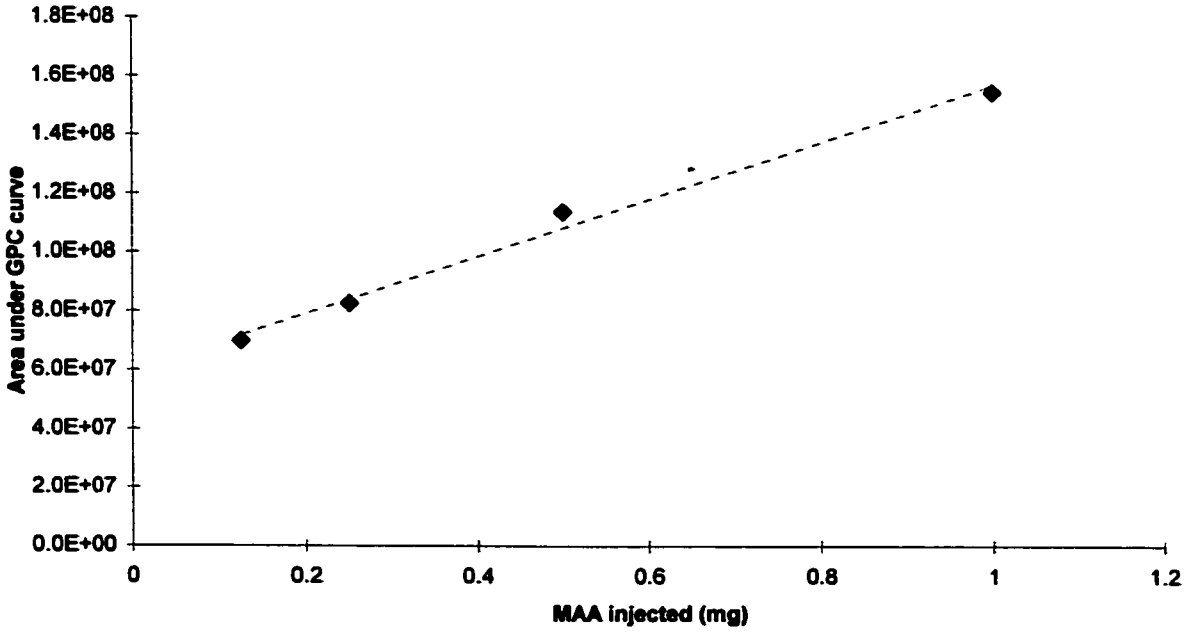

Figure 4.5: GPC Calibration Curve for Methacrylic Acid

A typical plot resulting from the GPC is shown in Figure 4.6. The first peak on the left corresponds to the macromonomer while the second peak from the left is that of the acid monomer. The areas under each peak correspond to the amount injected.

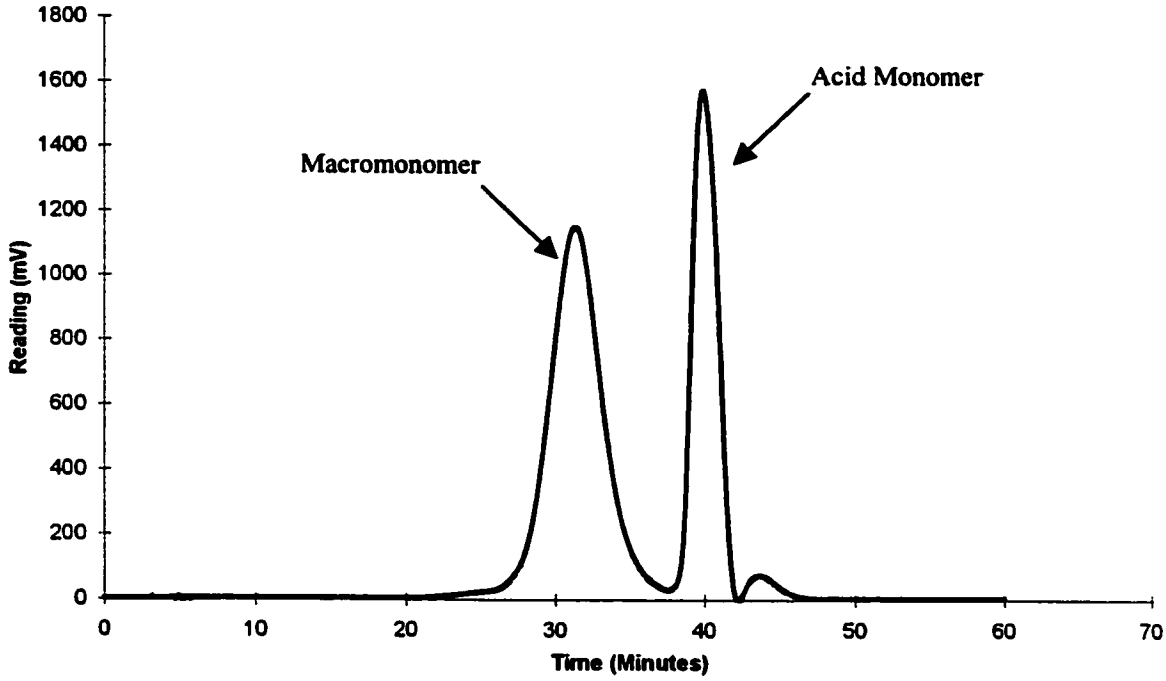

Figure 4.6: Typical GPC Curve for Residual Monomer Analysis

2) GPC Sample Preparation: After quenching the ampoule in an ice bath, the ampoule was opened using a cryogenic cut method. The cryogenic cut was performed with a glass cutting machine while the ampoule was at cryogenic temperature (T=-192°C). This cutting method was performed to avoid the evaporation of any monomer. After the ampoule was cut, it was stoppered and the mixture was then placed in a freezer for storage.

Before any further sample preparation, a certain amount of 0.45 micron disposable acrodisk filters were cleaned with 10 mL of THF. These filters were dried overnight (at least 24 hours) at low temperature (T = 40°C) under high vacuum. The filter washing step was necessary to remove the powder on the top of the filter, before using it to remove the polymer from the solution injected into the GPC.

On the next day, the weight of the mixing Erlenmeyer flask, the vial and the washed/dried filter were recorded. The ampoule contents were then thawed, well mixed and a recorded amount of reaction mixture was poured into the Erlenmeyer flask. THF was added to get a 10 or 15 mg/mL concentration of the reaction mixture. A 5 ml sample was taken into a filtration syringe and two acrodisk filters were attached to the syringe. The first filter was the washed/dried filter used to retain the copolymer. The second filter was used to filter the remaining solution. The filtration step took up to 3 hours and served to separate the polymer from the macromonomer and acid monomer.

After the filtration step was completed, the filtered solution was weighed and injected into the GPC. Reaction mixture samples of approximately 20 mg/mL in THF were injected into a Waters GPC equipped with a DRI 410 refractive index detector. An HR-3 Styragel column was used to achieve the sample fractionation at a flow rate of the THF carrier solvent of 0.1 mL/min. The acrodisk filters used to retain the polymer were placed into an oven at low temperature and high vacuum overnight to remove the remaining THF. After the GPC analysis, the area of the two peaks were integrated and recorded. The next day, the weight of the filter with the polymer was also recorded. It is noted that in some GPC solutions, a known weight of acid monomer was added, in order to bring the peak into a detectable range. In the calculation, this addition was taken into account. Since

the concentration of the original feed and of the reaction mixture were known, it was possible to obtain both the conversion and the polymer concentration from this analysis.

4.5 Experimental Methods for the Sty/BA system

For the Sty/BA system, reactivity ratio runs were performed using methods described in section 4.3. Identical methods were used for high conversion runs except that, of course, the reactions were allowed to proceed to higher conversion levels. In the case of the Sty/BA system, gravimetry was used to measure conversion, ^{1}H-NMR spectrometry was used to obtain the composition of the copolymer, and, for the high conversion runs only, GPC was used to measure the average molecular weights of selected samples. In addition, attenuated total reflectance Fourier-Transform infrared (ATR-FTIR) spectrometry was tested as an alternative means to measure the conversion and composition.

4.5.1 Design of Experiments

For the reactivity ratio estimation experiments, the initial compositions were calculated using the Tidwell-Mortimer criterion (see Section 3.4 and Tidwell and Mortimer, 1965). Initial guesses for the reactivity ratios were taken from the results of previous experiments by Dubé et al. (1991). The values used were: r_1=0.955 and r_2=0.183, where monomer 1 denotes styrene monomer and monomer 2 denotes butyl acrylate monomer. This gave initial styrene mole fractions of $f'_{10}=0.084$ and $f''_{10}=0.677$. As per the Tidwell-Mortimer criterion, repeat runs were performed at each of the feed

compositions. The reactivity ratio estimations were performed in bulk and in solution (at 50 wt.% toluene).

In the case of the high conversion runs, the initial compositions for the four sets of experiments were chosen to be equidistant in the styrene mass fraction range. The initial compositions chosen were 0.2, 0.4, 0.6 and 0.8 mass fraction of styrene. These runs were performed in 50 wt.% toluene solutions. This particular concentration was used to facilitate sample manipulation and analysis when using ATR-FTIR.

4.5.2 Gravimetry

The determination of conversion was obtained by gravimetry. The process of gravimetry involves the weights of both the monomer feed mixture and the final polymer product. The conversion of monomer to polymer was calculated using the following relation:

$$X = \frac{Weight(Dish + Polymer) - Weight(Dish)}{Weight(Ampoule + reactionMixture) - Weight(Ampoule)} * 100 = \frac{Weight(DriedPolymer)}{Weight(reactionMixture)} * 100 \quad (4.1)$$

A sample calculation is shown in Appendix C.

4.5.3 ^{1}H-NMR spectrometry

^{1}H-NMR spectra were obtained from the polymer samples, dried from the reaction mixtures. For each monomer a relative amount of each proton or group of protons is obtained at a specific wavelength. In the present case, the five protons on the benzene ring of the Sty absorb at approximately 6.5 ppm and the two protons of the methylene group closest to the oxygen in the ester portion of BA absorb at approximately 3.5 ppm.

from the area under the spectral peaks and from the formula of each monomer, it is possible to calculate the relative amounts of Sty and BA in the sample. A sample calculation is shown in Appendix C.

4.5.4 Gel Permeation Chromatography

GPC was used to determine the number- and weight-average molecular weights of selected samples. GPC analysis was performed with a Waters Associates GPC system equipped with three Waters Styragel-HR columns (10^3, 10^4 and 10^6 Å pore size) installed in series and a differential refractometer. Tetrahydrofuran was used as the mobile phase and was delivered at 0.3 mL/min. The amount injected was 10 μL and analysis time was 60 minutes. Calculations were performed using the Mark-Houwink coefficients for styrene and butyl acrylate averaged by polymer composition. The Mark-Houwink coefficients are shown in Table 4.1.

Table 4.1: Mark-Houwink Coefficients for GPC analysis

Monomer	K'	α'
Styrene	0.011	0.725
Butyl Acrylate	0.011	0.708

4.5.5 Attenuated Total Reflectance Infrared Spectrometry

Polymerization reactions were monitored off-line using an ATR-FTIR spectrometer, the ReactIR™ 1000 (ASI Applied Systems Inc.). It can be used to determine the overall conversion via the individual monomer conversion of each monomer. Details of the use of this probe for polymerization monitoring can be found elsewhere (Jovanovic and Dubé, 2001; Hua and Dubé, 2001; Hua and Dubé, 2002). The

analysis was done immediately after each ampoule was opened. Each ampoule was poured into a small glass vial and the ATR-FTIR probe was dipped into the reaction mixture. The vial was large enough so that the probe could be easily inserted. Then, infrared scanning was done and the computer collected the spectra after 64 scans, for almost 30 seconds of analysis. With the spectrum, the individual monomer conversion was determined by difference between the height of the sample peak and the raw mixture peak at the same wavelength. The height of the peak was determined using a two-point baseline correction method. After the height of the selected characteristic peak for each component was calculated, overall conversion was obtained by the two individual monomer conversions using the following equations:

$$x_1' = 1 - \frac{(Peak \cdot Height)_1 \, at \cdot time \cdot t}{(Peak \cdot Height)_1 \, at \cdot time \cdot 0} \tag{4.2}$$

$$X = \left[\frac{w_1}{w_1 + w_2} * x_1'\right] + \left[\frac{w_2}{w_1 + w_2} * x_2'\right] \tag{4.3}$$

where w_1 and w_2 are the weight fraction of monomer 1 and 2 and x_1' and x_2' are the individual monomer conversions. A sample calculation is shown in Appendix C.

After the ATR-FTIR analysis was done, the sample was poured immediately into a glass dish and the probe was washed three times using toluene. Ethanol was then added to the reaction mixture to precipitate the polymer. The probe was then washed again using acetone to make sure that the probe was clean. After the washing step, the probe was wiped using clean towels. An analysis of the ambient air was also performed to ensure that the probe was properly cleaned. The results of the ambient air analysis should be a baseline with no major peaks. If any peak occurred, the probe was rewashed.

Chapter 5

Results: Copolymerization of macromonomer / carboxylic acid monomer

5.1 First attempt: Separation with liquid-liquid extraction

Reaction conditions for the experiments conducted using post-polymerization method #1 (a total of 32 runs) are shown in Table 1.

Table 5.1: Molar feed compositions for runs using post-polymerization method #1

Ampoule Number	Macromonomer 1/AA	Ampoule Number	Macromonomer 2/AA	Ampoule Number	Macromonomer 1/MAA	Ampoule Number	Macromonomer 2/MAA
M1A1S1	0.0036	M2A1S1	0.0036	M1M1S1	0.0043	M2M1S1	0.0043
M1A1S2	0.0084	M2A1S2	0.0084	M1M1S2	0.0100	M2M1S2	0.0101
M1A1S3	0.0151	M2A1S3	0.0151	M1M1S3	0.0179	M2M1S3	0.0180
M1A1S4	0.0249	M2A1S4	0.0249	M1M1S4	0.0289	M2M1S4	0.0296
M1A1S5	0.0249	M2A1S5	0.0249	M1M1S5	0.0289	M2M1S5	0.0296
M1A1S6	0.0408	M2A1S6	0.0408	M1M1S6	0.0482	M2M1S6	0.0484
M1A1S7	0.0711	M2A1S7	0.0711	M1M1S7	0.0783	M2M1S7	0.0838
M1A1S8	0.1516	M2A1S8	0.1516	M1M1S8	0.1282	M2M1S8	0.1759

Note that due to the difference in monomer and macromonomer molecular weights, mole fractions are quite different from mass fractions.

Almost all of the runs listed in Table 1 were extremely reactive. In some cases the reaction were incontrollable. This problem arose once the polymerization went beyond a certain conversion level. Consequently, only very low conversion levels (conversions less than about 1%) were achievable. Otherwise, full conversion resulted and this was not useful for reactivity ratio estimation experiments. It is conceivable that only very small

small amounts of polymer were formed and this would explain the difficulties in the analysis and separation of the polymers from the comonomers.

While this post-polymerization method was largely unsuccessful, under more controlled conditions, where the rate of reaction can be held to a manageable level, this method may still yield reasonable results. In any case, we have not been able to confirm whether the method successfully separates macromonomer from polymer nor whether the saponification of acid groups can yield accurate polymer composition measurements using ^{13}C-NMR.

5.2 Second attempt: Separation with GPC

Reaction conditions and results for the experiments conducted using post-polymerization method #2 (a total of 24 runs) are shown in Tables 2 through 5. Each table contains the feed composition, and the wt.% conversion and copolymer composition from the GPC measurements.

Table 5.2: Experimental results for Macromonomer 1/MAA copolymerizations

Ampoule Number	Mole fraction macromonomer in feed	Conversion (wt.%)	Mole fraction macromonomer in copolymer
M1M2S1	0.028	15.90	0.008
M1M2S2	0.041	16.17	0.008
M1M2S3	0.067	32.20	0.010
M1M2S4	0.114	27.89	0.021
M1M2S5	0.230	48.03	0.012
M1M2S6	0.448	62.04	0.058

Table 5.3: Experimental results for Macromonomer 2/MAA copolymerizations

Sample Number	Mole fraction macromonomer in feed	Conversion (wt.%)	Mole fraction macromonomer in copolymer
M2M2S1	0.023	14.28	0.019
M2M2S2	0.035	19.94	0.012
M2M2S3	0.057	57.87	0.046
M2M2S4	0.097	28.44	0.021
M2M2S5	0.202	20.60	0.032
M2M2S6	0.402	38.46	0.098

Table 5.4: Experimental results for Macromonomer 1/AA copolymerizations

Sample Number	Mole fraction macromonomer in feed	Conversion (wt.%)	Mole fraction macromonomer in copolymer
M1A2S1	0.191	85.29	0.054
M1A2S2	0.231	78.87	0.034
M1A2S3	0.279	78.89	0.052
M1A2S4	0.347	76.60	0.063
M1A2S5	0.448	76.69	0.070
M1A2S6	0.616	81.72	0.061

Table 5.5: Experimental results for Macromonomer 2/AA copolymerizations

Sample Number	Mole fraction macromonomer in feed	Conversion (wt.%)	Mole fraction macromonomer in copolymer
M2A2S1	0.169	72.67	0.051
M2A2S2	0.201	80.50	0.067
M2A2S3	0.245	73.01	0.055
M2A2S4	0.303	61.14	0.035
M2A2S5	0.402	44.26	0.025
M2A2S6	0.579	43.89	0.026

It is evident from Tables 2 through 5 that very little macromonomer was bound into the copolymer. There are three possible explanations for this. The first is that perhaps the GPC analysis was incorrect. Recall that the GPC analysis was performed on residual monomer. The results could be indicating that a large proportion of the residual

macromonomer was being trapped during the sample filtering process. While this is entirely possible, it would seem unlikely, in light of the fact that the samples were fairly dilute. A second explanation might be that the macromonomer reactivity ratios, r_1, are very close to zero and hence, the macromonomer is not being incorporated in the copolymer. Since, there doesn't appear to be much change in the copolymer composition even for higher conversion samples, this also seems unlikely. The third possible explanation for the low macromonomer content in the copolymers is that the reaction mixture has become somewhat heterogeneous as the polymerization proceeds. This heterogeneity would perhaps cause most of the macromonomer to be in a different phase than the free radicals and thus not participate to a great extent, if at all, in the copolymerization.

5.3 Reactivity Ratio Estimation using RREVM

The results from table 2 through 5 were each incorporated into the RREVM program (Polic et al., 1998, Dubé et al., 1997). The RREVM program exhibited some numerical instability and either negative reactivity ratios were estimated or the program failed to converge to a value.

These results tend to support the idea that the reactivity ratios are very close to zero or that homo- as opposed to copolymers are being formed. The study was halted at this point. The scope of the project did not allow us to continue the study.

Chapter 6

Results for the Styrene/Butyl Acrylate system

6.1 Low Conversion Styrene/Butyl Acrylate Copolymerization

Results for low conversion Sty/BA copolymerization in bulk and solution are shown in Tables 6.1 and 6.2, respectively. Detailed data for these experiments are available in Appendix A.

Table 6.1: Reactivity Ratio Estimation Runs for Bulk Copolymerization

Ampoule Number	Monomer Feed Composition (Styrene mol fraction)	Polymer Composition (Styrene mol fraction)	Conversion (wt.%)
BC1	0.677	0.696	7.72
BC2	0.677	0.705	5.13
BC3	0.677	0.697	5.37
BC4	0.677	0.690	5.23
BC5	0.084	0.260	3.17
BC6	0.084	0.263	3.93
BC7	0.084	0.259	3.28

Table 6.2: Reactivity Ratio Estimation Runs for Solution Copolymerization

Ampoule Number	Monomer Feed Composition (Styrene mol fraction)	Polymer Composition (Styrene mol fraction)	Conversion (wt.%)
SC1	0.677	0.711	3.12
SC2	0.677	0.707	3.06
SC3	0.677	0.713	3.16
SC4	0.677	0.714	3.11
SC5	0.084	0.267	1.68
SC6	0.084	0.274	1.28
SC7	0.084	0.268	2.01

Reactivity ratios were estimated from the low conversion data in Tables 6.1 and 6.2 using the RREVM software (Polic et al. 1998, Dubé et al. 1991). Results obtained for bulk copolymerization were: $r_1 = r_{Sty} = 0.7183$ and $r_2 = r_{BA} = 0.1849$; and for solution copolymerization were: $r_1 = r_{Sty} = 0.7966$ and $r_2 = r_{BA} = 0.1744$.

A 95% posterior probability contour plots were generated and plotted with reactivity ratios from the literature in Figure 6.1. It is seen that the 95% posterior probability contour plot from bulk and solution copolymerization very slightly intersect. This would imply that no significant solvent effects are manifested on the reactivity ratios.

Observation of Figure 6.1 leads to the conclusion that the reactivity ratios obtained from this study are comparable to that of the literature. The reactivity ratios from the literature were previously listed in Table 2.2. It is interesting to note the narrow range for the r_2 values compared to the broad range of values for r_1. This result was also reflected by the shape of the 95 % posterior probability contours. In view of this spread of data, solvent effects on composition are likely to be difficult to detect from these data. There is suspicion that penultimate unit effects may also be active for Sty/BA copolymerization (Dubé et al., 1990). If such is the case, then attempts to estimate reactivity ratios based on the Mayo-Lewis model (a.k.a. terminal model) kinetics may be ill-advised. This could account for the spread in the r_1 estimates. However, to date, no conclusive evidence for penultimate unit effects on Sty/BA composition has been shown, although effects on the rate are strongly supported (Ziaee and Nekoomanesh, 1998). The high conversion data to follow, can offer more insight into the effect of solvent.

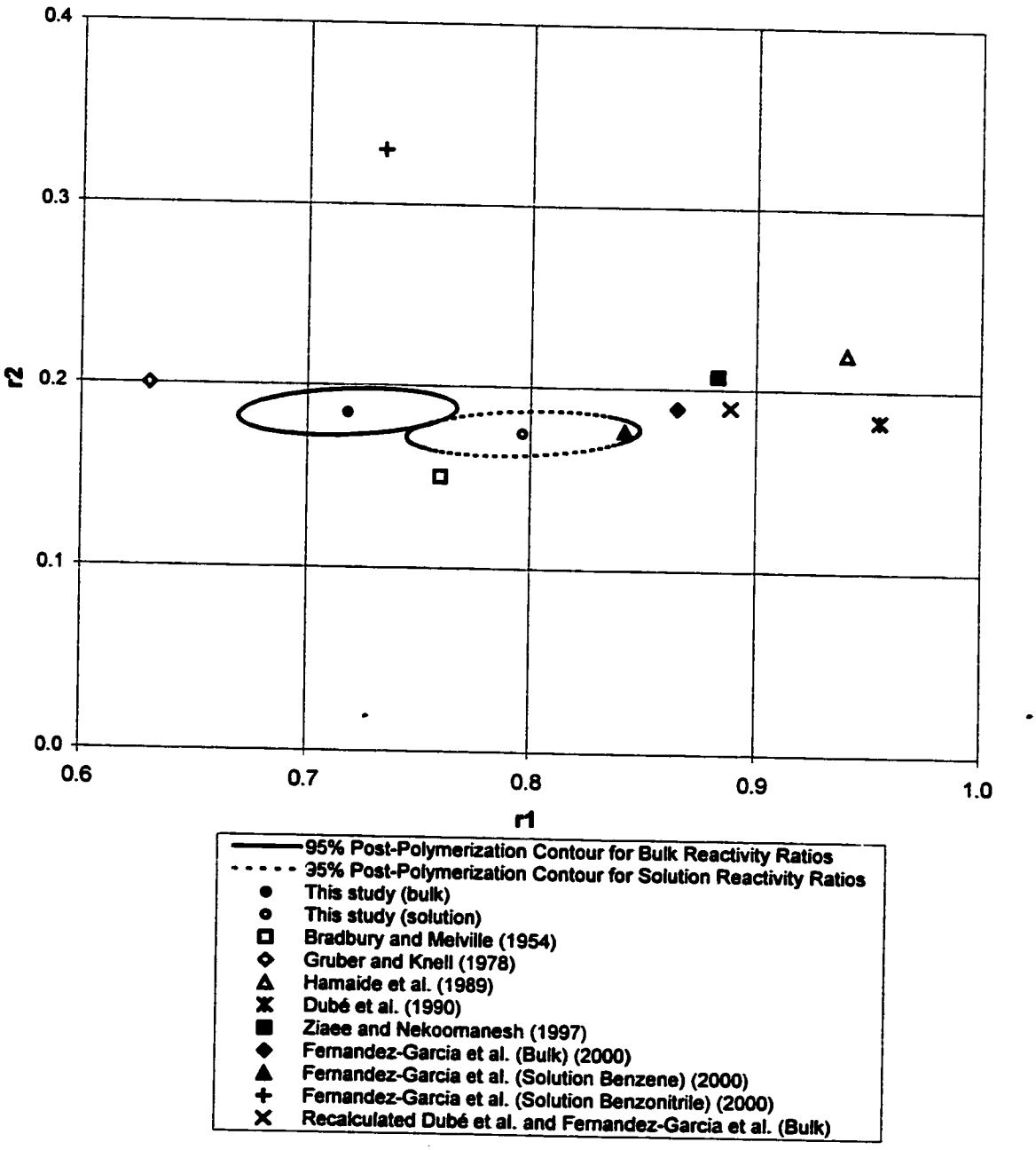

Figure 6.1: Sty/BA Bulk & Solution Reactivity Ratios

6.2 High conversion Sty/BA Copolymerization

Figure 6.2 gives the conversion versus time plot for all of the high conversion runs. This plot shows that an increasing amount of styrene in the reaction mixture increases the time necessary to reach full conversion. For the 40, 60 and 80 wt.% styrene cases, the data show only slight differences. For the 20 wt.% styrene case, the reaction mixture reaches full conversion in a shorter time. This behavior is due to the fact that butyl acrylate adds more rapidly to the polymer chain compared to styrene as indicated by the reactivity ratios.

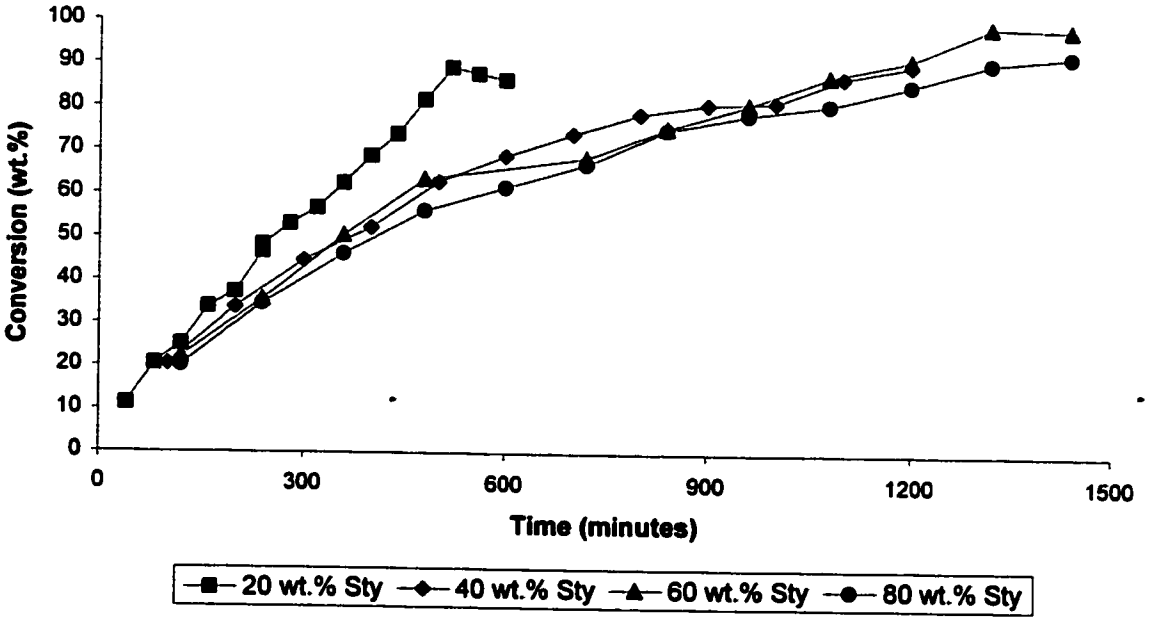

Figure 6.2: High Conversion Runs, Conversion versus Time

Figures 6.3 through 6.6 give the composition versus conversion data for each run. The first plot shows a high composition drift throughout the polymerization reaction. The drift is about 35% for the 20 wt.% styrene run. This value is very high compared to the other experiments with higher styrene feed contents (Figure 6.6). The reason for this is

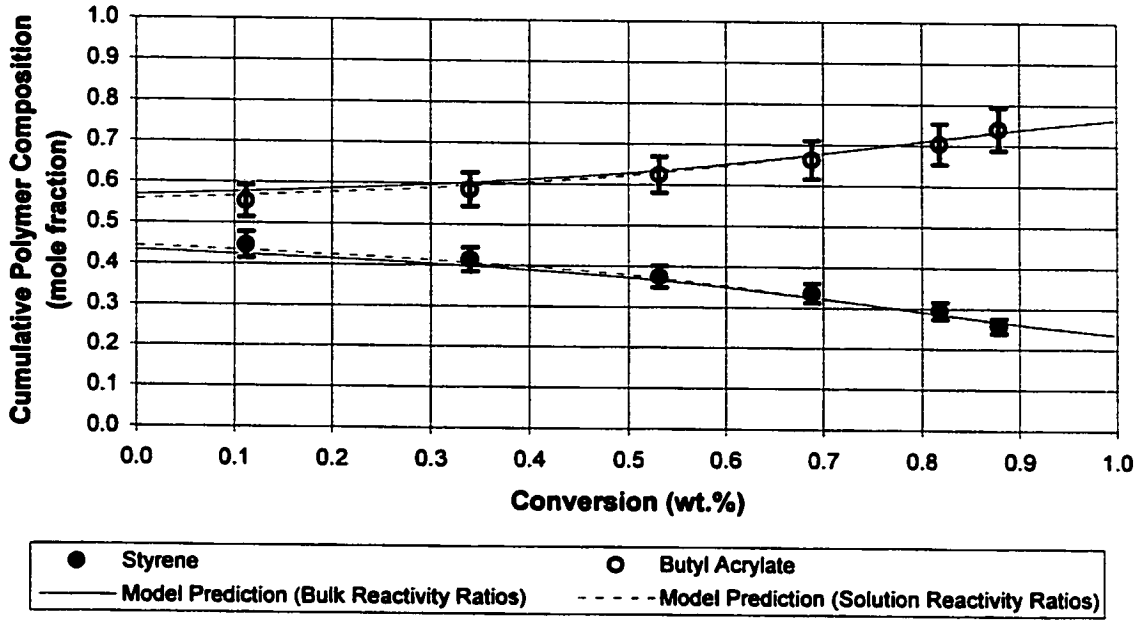

Figure 6.3: Sty/BA Composition vs Conversion (20 wt.% Sty)

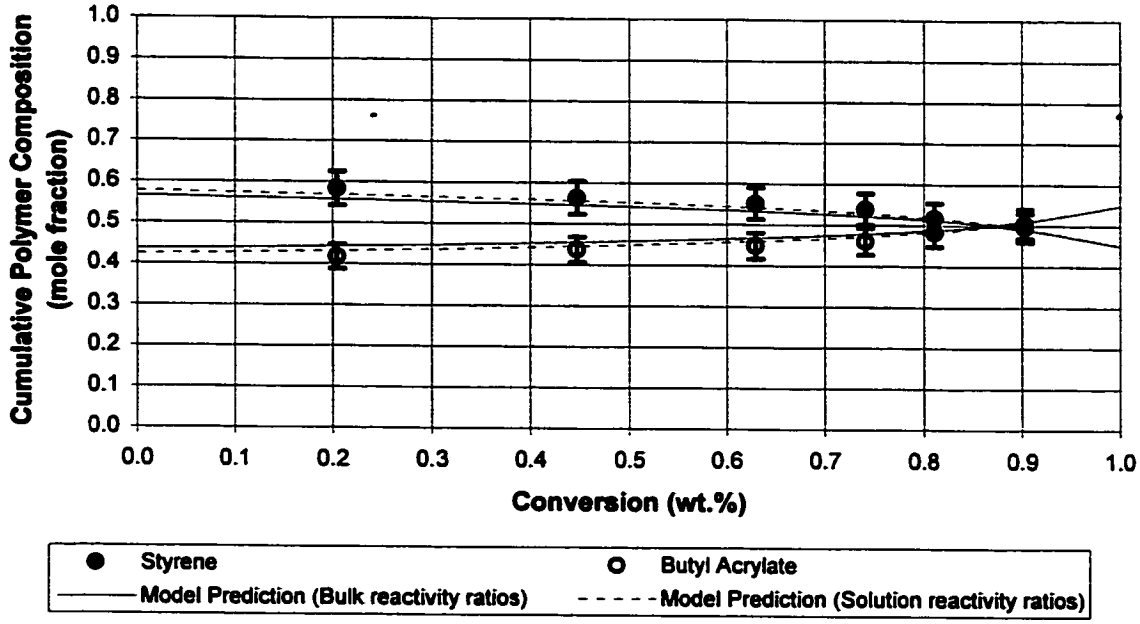

Figure 6.4: Sty/BA Composition vs Conversion (40 wt.% Sty)

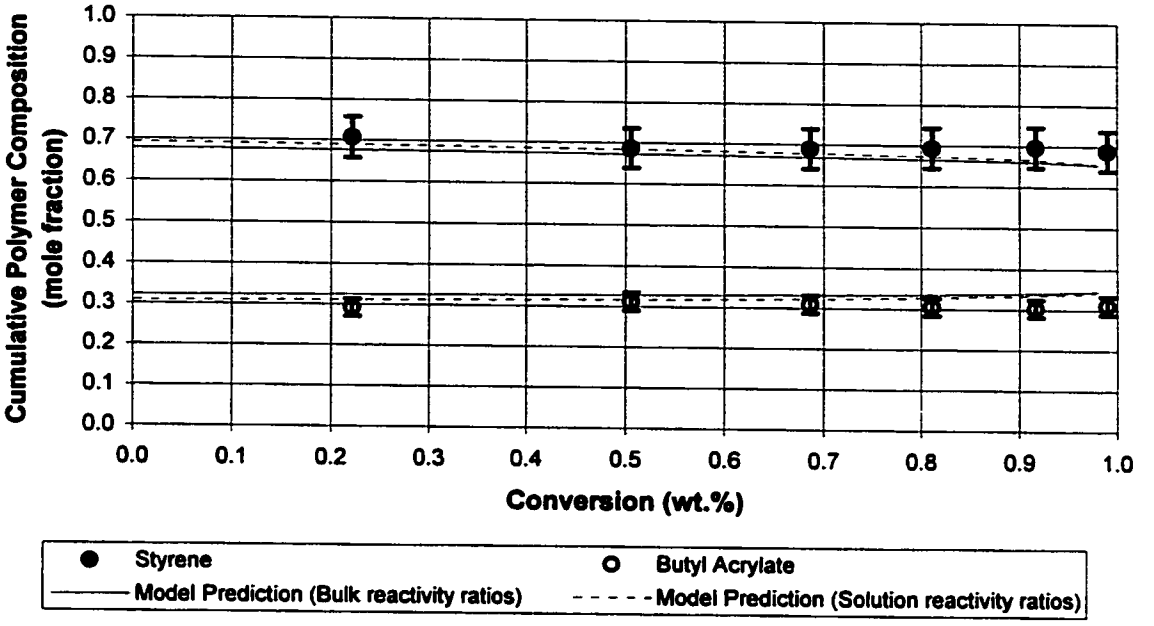

Figure 6.5: Sty/BA Composition vs Conversion (60 wt.% Sty)

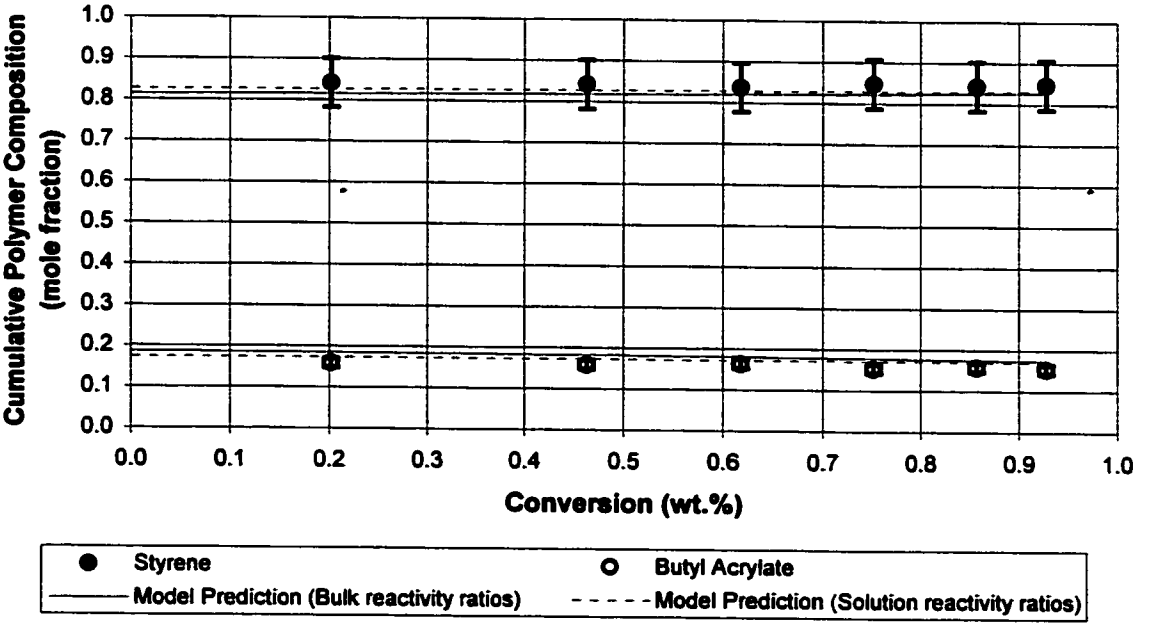

Figure 6.6: Sty/BA Composition vs Conversion (80 wt.% Sty)

that the monomer feed composition (80 wt.%) was near the azeotropic composition. The azeotropic composition is the composition where the polymers formed have the same composition as the feed. In the present study, the azeotropic composition is: 0.8023. Calculation of the azeotrope is given in Appendix C.

In each of Figures 6.3 to 6.6, model predictions based on the Mayo-Lewis or terminal model are given. These predictions were calculated from a model developed by Badeen (2000). Predictions using either the bulk reactivity ratios (i.e. r_1=0.7183, r_2=0.1849) or the solution reactivity ratios (i.e. r_1=0.7966, r_2=0.1744) are shown. It is evident from these predictions that polymer composition is well predicted by either set of reactivity ratios. This supports the comments in section 6.1 that solvent has an effect on polymer composition. Furthermore, it appears that the terminal model is sufficient for predicting polymer composition.

Weight-average molecular weights for selected samples are plotted in Figure 6.7 versus conversion. Relatively low molecular weights (< 30,000) were measured. This is expected as the reactions were performed in solution. First of all, due to the effect of dilution, the rate of polymerization and thus, the molecular weights will be reduced. Secondly, toluene solvent will participate as a chain transfer agent (see section 3.2.1) and will also contribute to the lowering of molecular weight. Finally, the purposeful addition of a CTA also served to reduce the molecular weight. Comparing all 4 runs, only the case with 20 wt.% Sty appears to differ significantly in terms of its molecular weight. This was earlier reflected in Figure 6.2 in terms of conversion rate. This difference can be attributed to the effect of BA, which is known to undergo chain transfer to polymer reactions (see section 3.2.2), which drives the molecular weight higher. This result was

also reflected in the polydispersity of the final sample of 2.47 for this run, while for the other runs, it was around 2. Results for the number-average molecular weight and polydispersity are shown in Appendix A.

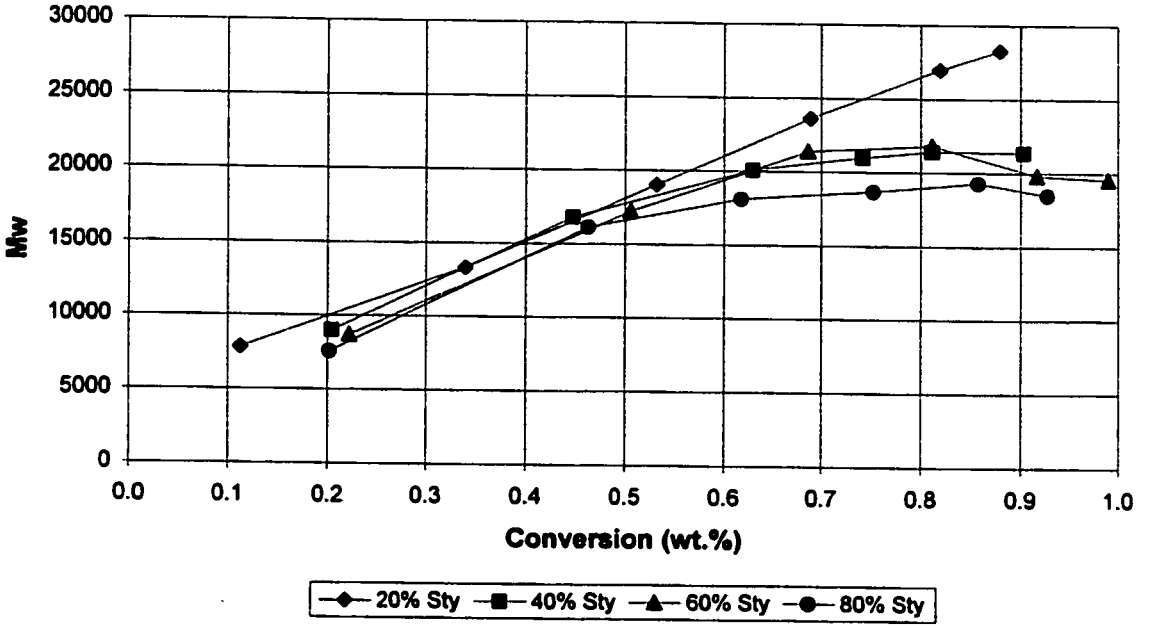

Figure 6.7: Weight-Average Molecular Weights

It is interesting to see the raw molecular weight distribution curves from GPC for each run. Those for the 20 wt.% Sty run are plotted in Figure 6.8; those for the remaining runs are shown in Appendix D. In Figure 6.8, one can observe a low molecular weight shoulder at the early stages of the reaction. As the reaction proceeds, the shoulder is greatly reduced and finally, a broad molecular weight distribution is shown. Each run exhibited a similar trend.

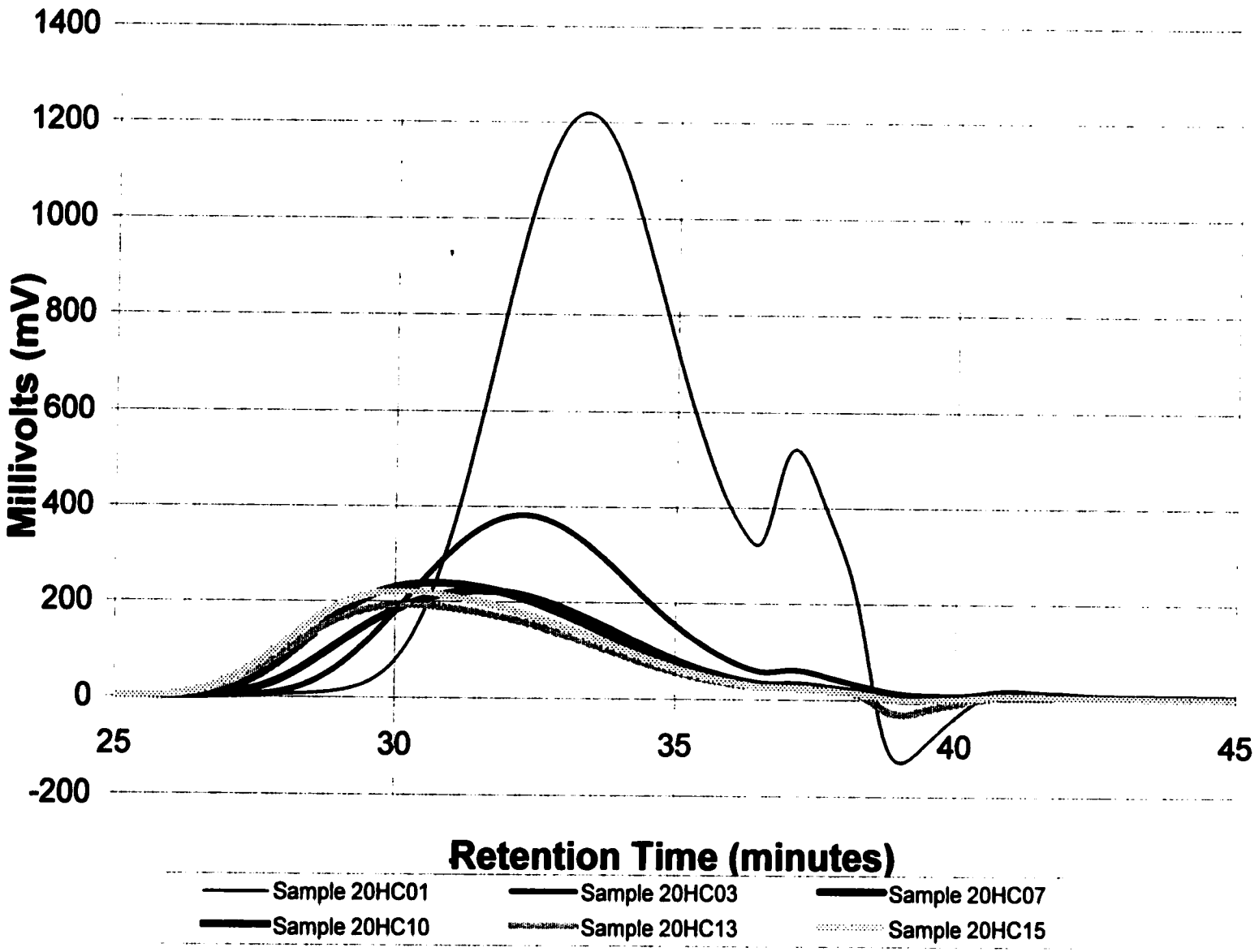

Figure 6.8: GPC Curves for high conversion runs at 20 wt.% Styrene

6.3 ATR-FTIR Spectrometry Results

ATR-FTIR spectrometry has been shown to be a very promising method for conversion and composition determination in many systems (Jovanovic and Dubé, 2001; Hua and Dubé, 2001, Hua and Dubé, 2002). The method has not been tested on the styrene/butyl acrylate system. One goal of this work was to test ATR-FTIR spectrometry to obtain the conversion and the composition of the Sty/BA system and to validate it with gravimetric and ^{1}H-NMR spectrometry results.

The results obtained from ATR-FTIR spectrometry are highly dependent on the selection of a characteristic peak for each monomer. Some guidelines are listed in various handbooks on the peak assignment of styrene and butyl acrylate monomer and homopolymers. The peak assignments useful to this work are listed in Tables 6.3 and 6.4.

By looking at the monomer peak assignments, we can easily determine which wavelength must be compared to get each individual monomer conversion. Figures 6.9 to 6.12 show ATR-FTIR spectra for the pure components (i.e. toluene, styrene, and butyl acrylate) and a sample reaction mixture, respectively. The two monomer peaks should not interfere each other and should not interfere with its corresponding polymer. In the present case, the two wavelengths chosen were: 773.7 cm^{-1} for styrene monomer representing the C-H ring wag and 810 cm^{-1} for butyl acrylate monomer representing the $=CH_2$ twist. The use of the peak for BA at 810 cm^{-1} was used previously in our laboratory (Hua and Dubé, 2001). In some cases, the monomer can overlap with the pure toluene spectrum. In those cases, the peak should not be chosen or the toluene spectrum should be subtracted from the overall spectra using the ReactIR software. In the present case, the two peaks chosen for the

ATR-FTIR analysis did not interfere with the pure toluene spectrum. Detailed results from the ATR-FTIR spectrometry are given in Appendix B.

Table 6.3: Peak Assignment for Styrene Monomer and Homopolymers

Styrene Monomer		Polystyrene	
Spectral Region (cm^{-1})	Absorbance Assignment	Spectral Region (cm^{-1})	Absorbance Assignment
3081	$=CH_2$ stretching		
3060	Ring C-H stretching vibration	3028	Ring –CH stretching
3027	Ring C-H stretching vibration		
3010	-CH= stretching	2927	$-CH_2$ asymetric stretching
1630	C=C stretching	2858	$-CH_3$ asymetric stretching
1602	Ring quadrant stretching	1599	Ring quadrant stretching
1576	Ring quadrant stretching		
1495	Ring semi-circle stretching	1491	Ring semi-circle stretching
1449	Ring semi-circle stretching	1452	Ring semi-circle stretching
1412	$=CH_2$ deformation	1367	$-CH-CH_2$ wag
1202	C-CH= stretching	1166	$-CH-CH_2$ wag
1082	Ring semi-circle stretching	1066	Ring semi-circle stretching
1021	Ring semi-circle stretching	1027	Ring semi-circle stretching
991.8	-CH= wag		
906.9	$-CH_2$ wag		
773.7	Ring C-H wag	758	Ring C-H wag
696.6	Ring bending	695.1	Ring bending

Table 6.4: Peak Assignment for Butyl Acrylate Monomer and Homopolymer

Butyl Acrylate Monomer		Polybutyl Acrylate	
Spectral Region (cm^{-1})	Absorbance Assignment	Spectral Region (cm^{-1})	Absorbance Assignment
2950-2850	Aliphatic C-H stretching	3000-2800	Methyl, methylene and methane C-H stretching
1725	C=O stretching	1740	C=O stretching
1638-1621	Acrylate C=C doublet		
1466	C-H deformation in methyl and methylene bands	1470	C-H deformation in methyl and methylene bands
1409	C-H deformation in $=CH_2$		
1273	=CH rock	1400-1300	C-H deformation in $C-CH_3$ band
1187	$=C-(C=O)-O-CH_2-$ stretching of aliphatic ester bands	1270-1150	$=C-(C=O)-O-CH_3$ stretching of aliphatic ester bands
1063	$=CH_2$ rock		
984	Trans =CHR wag		
967	$=CH_2$ wag		
810	$=CH_2$ twist		
668	C=O wag	486	C=O wag

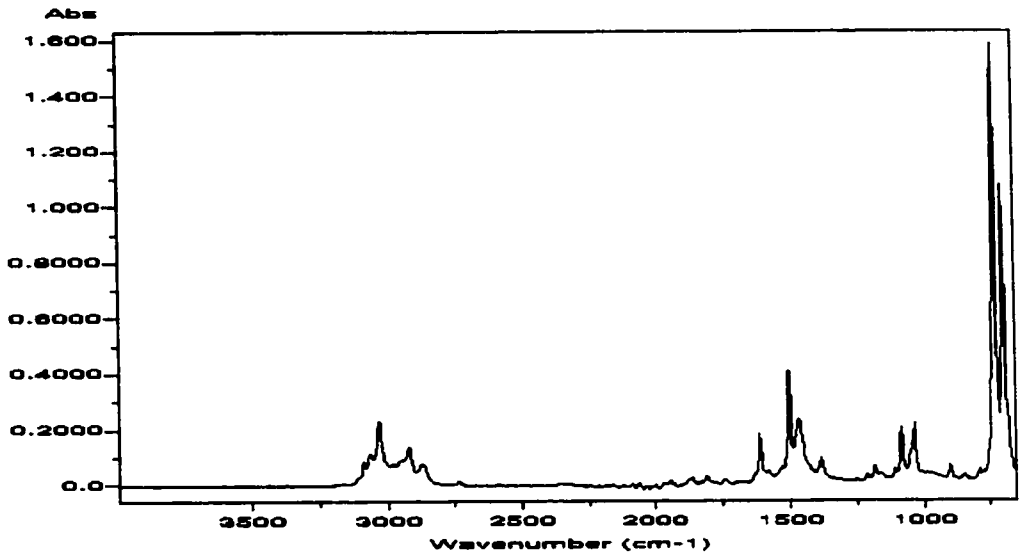

Figure 6.9: ATR-FTIR Spectra of Pure Toluene

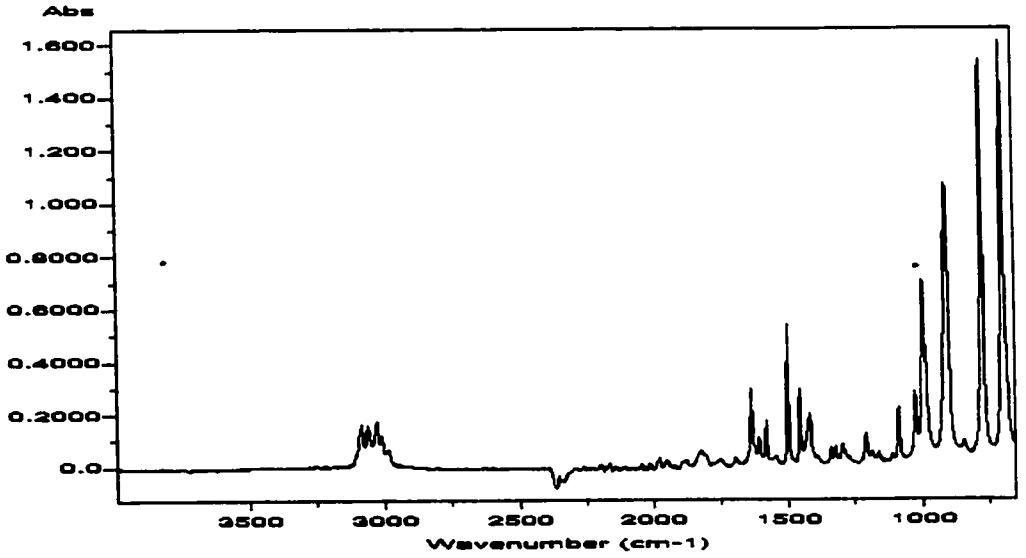

Figure 6.10: ATR-FTIR Spectra of Pure Styrene

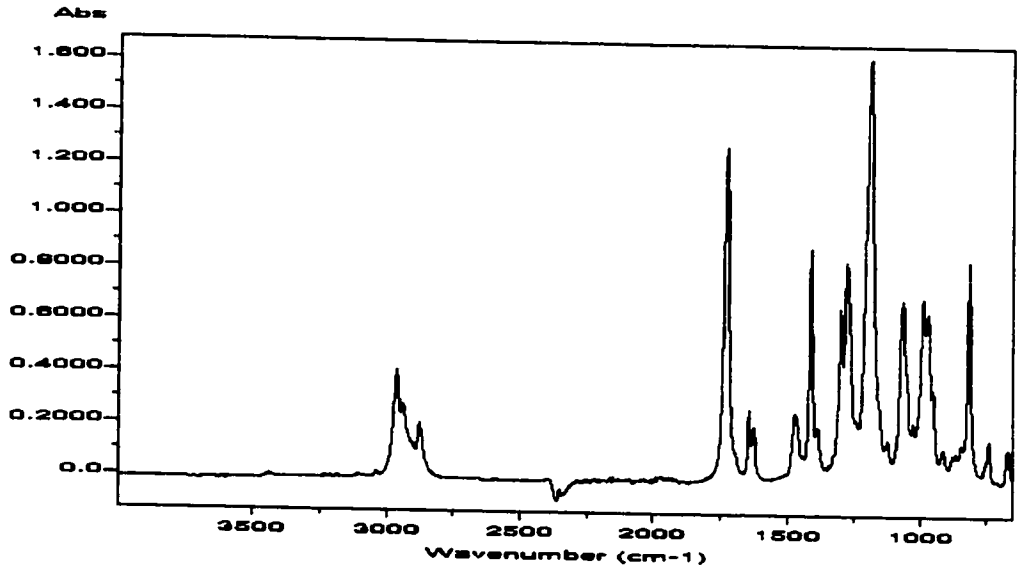

Figure 6.11: ATR-FTIR Spectra of Pure Butyl Acrylate

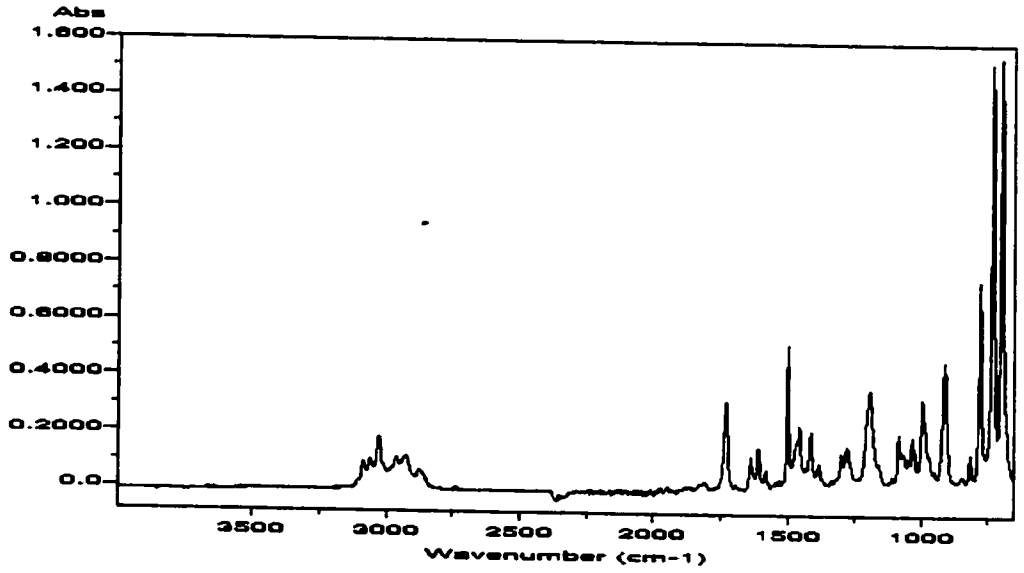

Figure 6.12: Typical ATR-FTIR Spectra of a Reaction Mixture Sample

With the peak wavelengths chosen, individual monomer conversions were determined using equation 4.2 in section 4.5.5. The heights of each peak were calculated using a two-point baseline method (see section 4.5.5). The results are presented in Figures 6.13 to 6.16. The data given in the figures are the overall conversion and the individual conversions from both ATR-FTIR spectrometry and gravimetry combined with ^{1}H-NMR spectrometry. Open symbols in the figures represent results from ATR-FTIR whereas closed symbols represent gravimetric and ^{1}H-NMR spectrometry results. Sample calculations are shown in Appendix C. Figure 6.13 through figure 6.15 additionally shows the error bars for the ATR-FTIR spectrometry results. Based on these error estimates, the ATR-FTIR spectrometry data are not significantly different than the gravimetric and ^{1}H-NMR spectrometry results. The percentage error in the peak height reading is 2.46 %. In the same manner, the percentage error of the balance used for the gravimetry calculation is 0.0005 and the error on the ^{1}H-NMR spectrometry is 5%. The error bars are represented in figure 6.13 through 6.15. The error bars are similar for each of Figures 6.17 through 6.19.

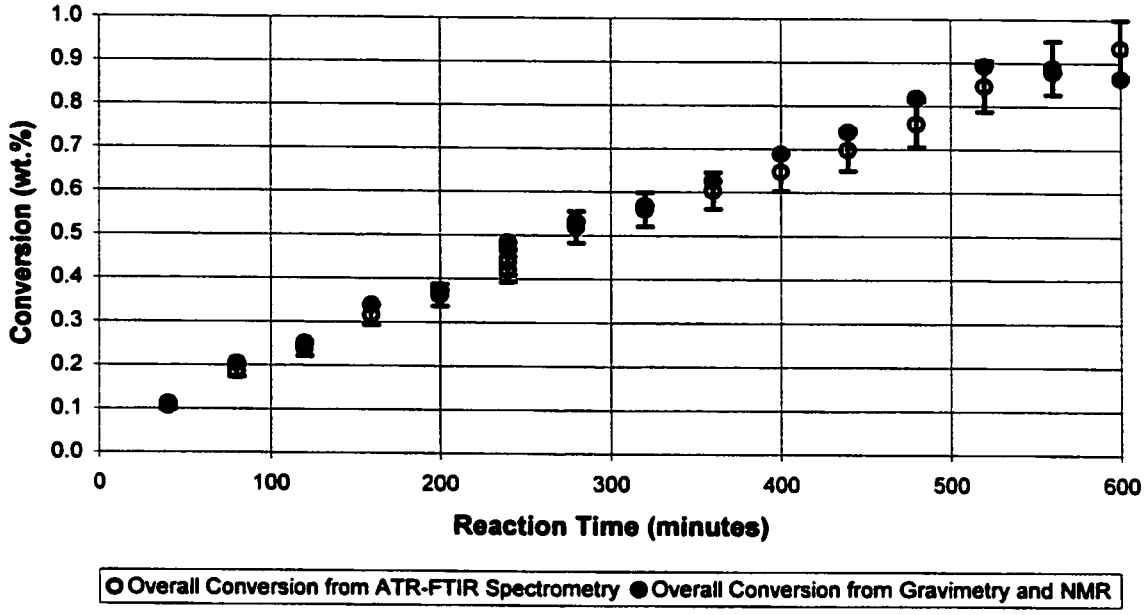

Figure 6.13: Error Bars for Overall Conversion for the 20 wt.% Styrene Runs

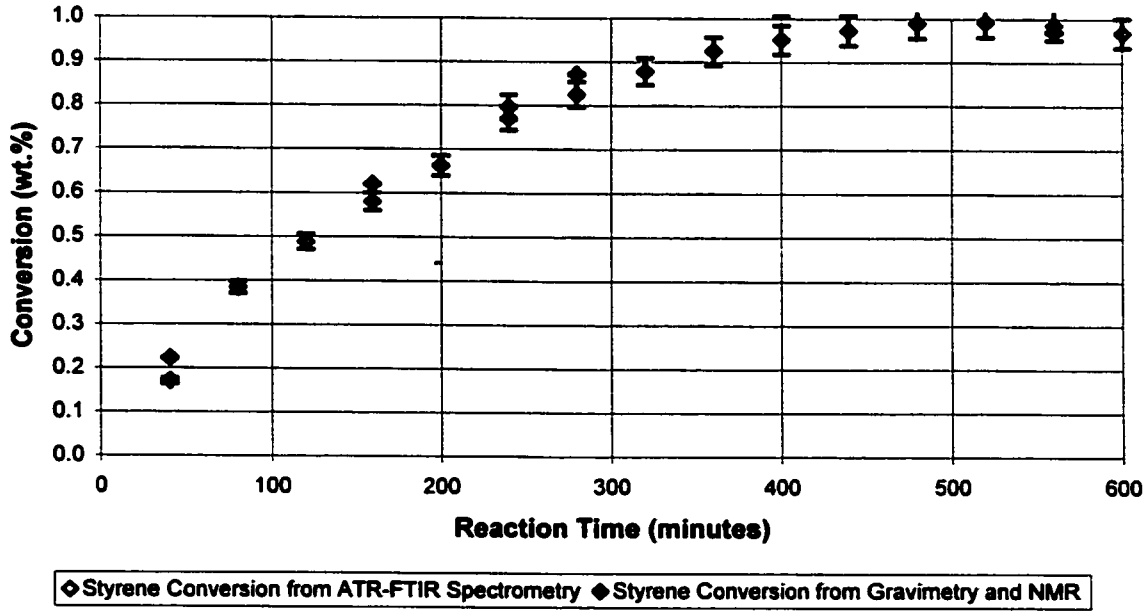

Figure 6.14: Error Bars for Styrene Conversion for the 20 wt.% Styrene Runs

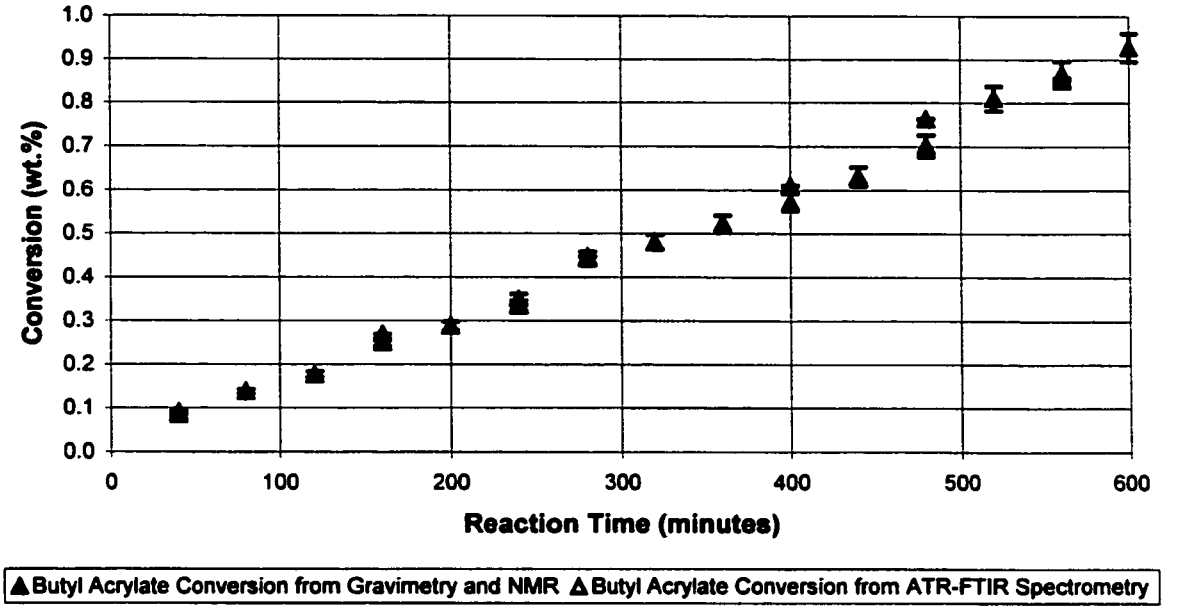

Figure 6.15: Error Bars for Butyl Acrylate Conversion for the 20wt.% Styrene Runs

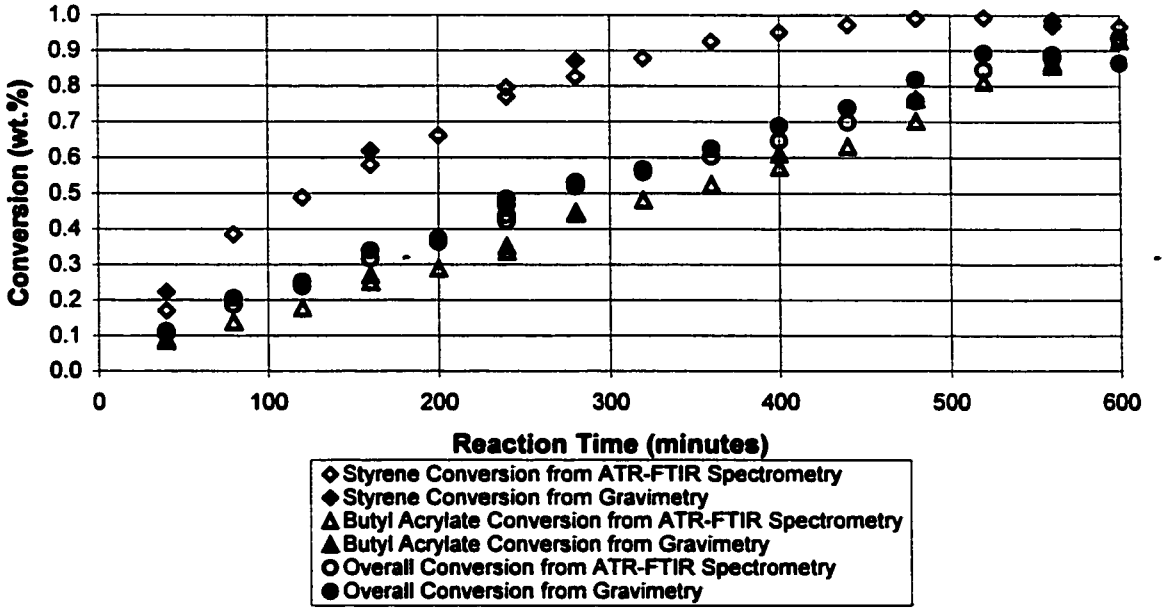

Figure 6.16: ATR-FTIR Results compared to Gravimetry for 20 wt.% Styrene

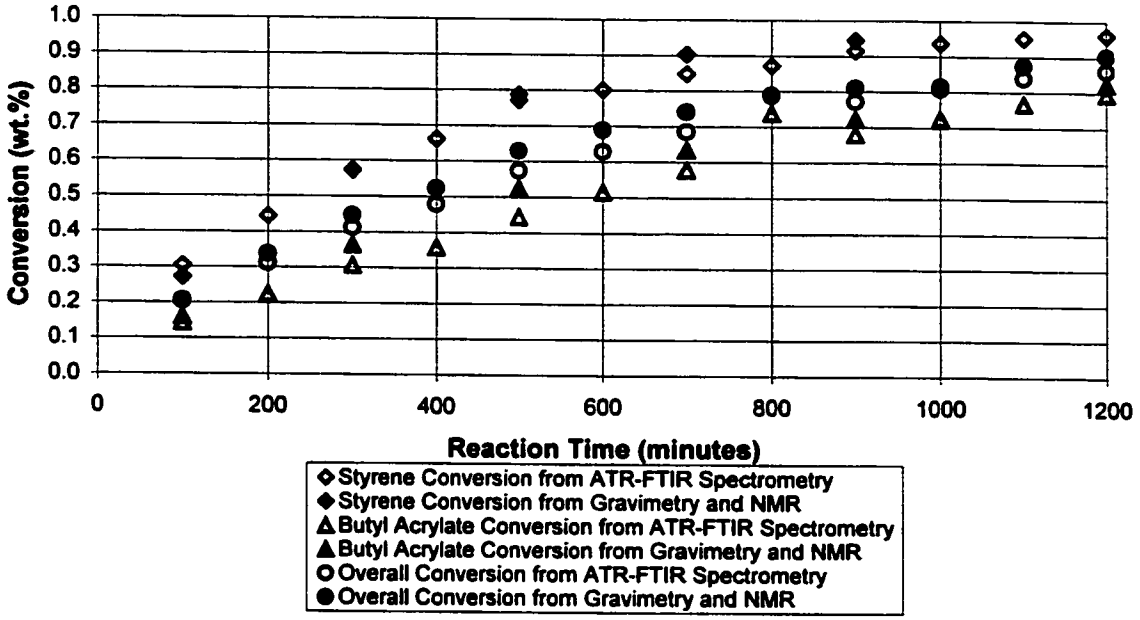

Figure 6.17: ATR-FTIR Results compared to Gravimetry for 40 wt.% Styrene

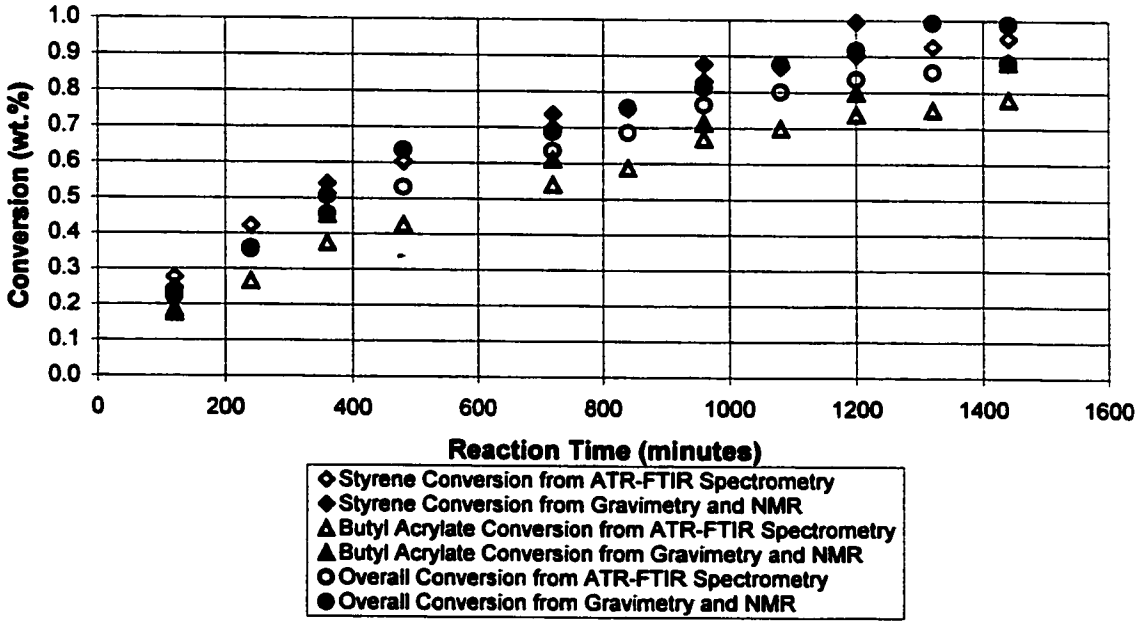

Figure 6.18: ATR-FTIR Results compared to Gravimetry for 60 wt.% Styrene

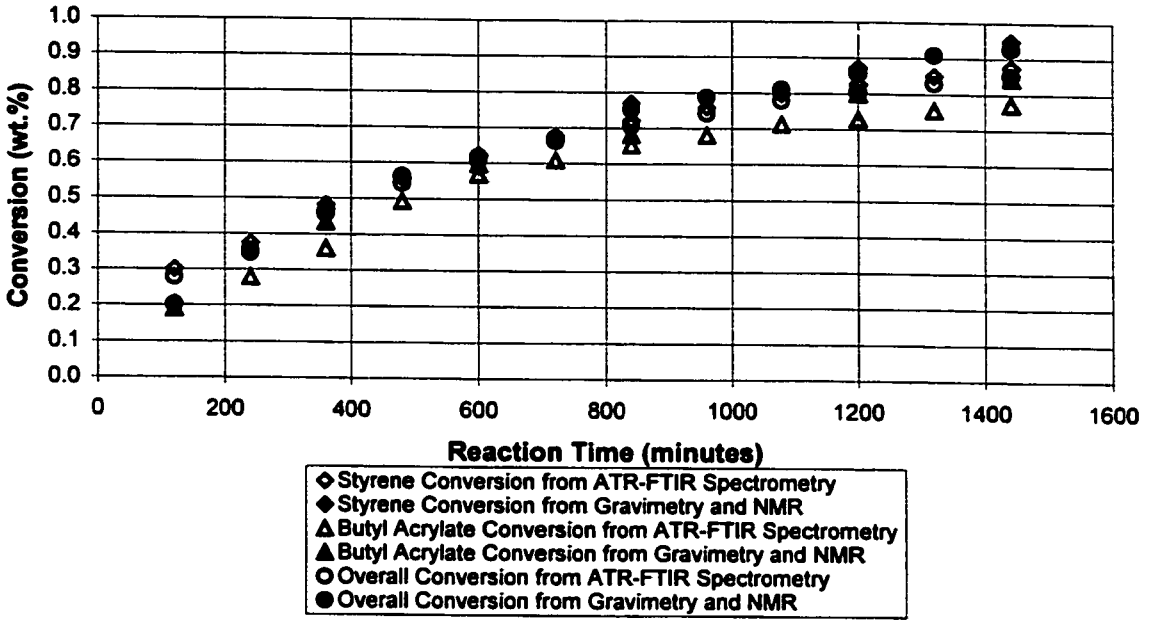

Figure 6.19: ATR-FTIR Results compared to Gravimetry for 80 wt.% Styrene

Despite the lack of significant differences in the results between the ATR-FTIR spectrometry and the traditional off-line techniques, in Figures 6.16 to 6.19, the ATR-FTIR results consistently underestimate the results from the standard techniques. In addition, the differences between the results are somewhat independent of the monomer feed composition. Interference from the toluene solvent is therefore ruled out. One possible hypothesis is that the styrene and the butyl acrylate peaks are slightly interfering with each other. This would explain how in cases when one monomer dominates the composition (i.e. Figures 6.16 and 6.19), results are reasonably good; whereas, when more or less equal amounts of monomer are present (i.e. Figures 6.17 and 6.18), the differences are more pronounced. Figure 6.20 shows the characteristic peaks of interest for several pure monomer mixtures. This figure shows the two peaks of interest: the first one, at 810.4 cm^{-1}, is the butyl acrylate peak and the second one, at 773.7 cm^{-1}, is the styrene peak. There is some slight interference between the peaks at ~795 cm^{-1}. This

interference is more pronounced when both monomers are present in substantial amounts. Thus, at composition extremes, one would expect less interference in contrast to when more or less equal amounts of both monomers are present. This, in particular, makes the establishment of the baseline difficult. Because of the difficulties with the characteristic peaks used above, other alternative peaks were tried but results were even less promising.

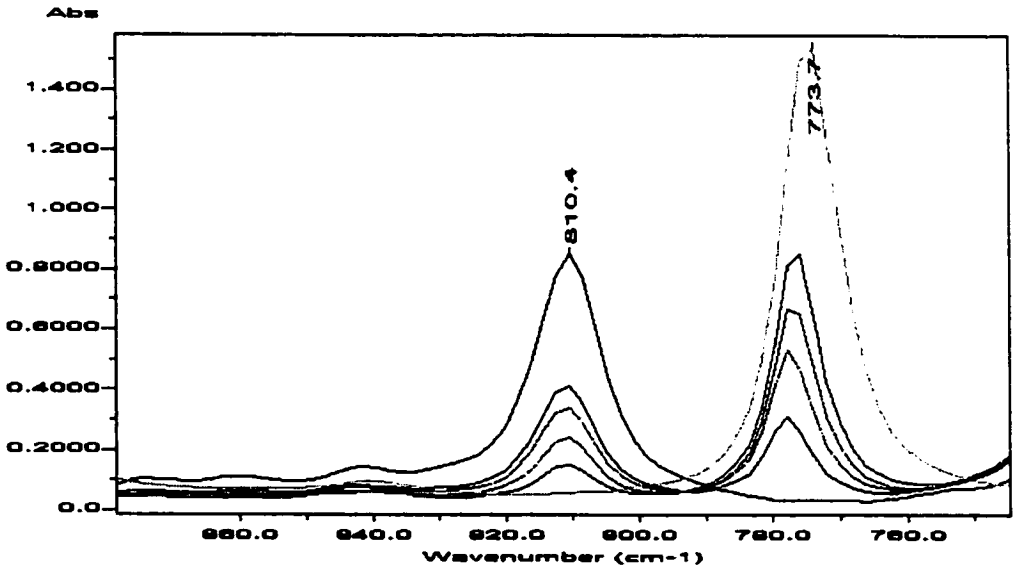

Figure 6.20: ATR-FTIR Spectra for Pure Monomer Mixture

A future goal is to increase our ability to monitor Sty/BA emulsion polymerizations in-line. The difficulties encountered in the present case, may improve only slightly because the solvent, which would be replaced by water in the emulsion polymerization will showing only a slight interference with the spectra.

Chapter 7

Conclusions and Recommendations

7.1 Conclusions

7.1.1 Macromonomer/Carboxylic Acid Monomer Experiments

For the estimation of reactivity ratios, three measured quantities are needed from a polymerization experiment at a conversion less than 100%. Obviously, one requires both the feed composition and the polymer composition (both are often expressed as mole fractions). In addition, if one operates at conditions where composition drift is negligible (<5%), then knowing the conversion precisely is not completely necessary. However, in cases where composition drift may be significant, the conversion should be known precisely.

For the copolymer system involving the macromonomer, we have tried to address the issue of measuring the polymer composition and conversion. Due to the difficulty of the residual monomer separation from the polymer, both the conversion and the composition were not easily obtainable through traditional techniques (i.e. gravimetry and ^{1}H-NMR spectrometry). Instead, they were obtained using GPC to measure the amounts of residual monomers. Using that method, both polymer composition and conversion were measured. The issue, in this case, was the solubility of the macromonomer and acid monomers. Hence, questions regarding the exclusion of macromonomer from the injected sample during the sample filtration step were raised. Thus, if the polymer can also be dissolved and injected into the GPC, the confidence in

the measured results will greatly increase. Unfortunately, in this case, results were inconclusive.

7.1.2 Styrene/Butyl Acrylate Monomer Experiments

In this system, the reactivity ratio estimation posed few challenges. The results obtained for the reactivity ratios were close to that in the literature. The results obtained in this work were for bulk copolymerization: $r_1 = 0.7183$ and $r_2 = 0.1849$; and for solution copolymerization: $r_1 = 0.7966$ and $r_2 = 0.1744$.

Based on the reactivity ratio values and 95% posterior probability contour plots, solvent effects on the reactivity ratios appeared to be slight. However, high conversion experiments revealed no significant solvent effects on the polymer composition. Nonetheless, solvent did have an impact on the copolymerizations. A dilution effect and a chain transfer effect were in evidence in the polymerization rate data and relatively low molecular weights were produced.

As the monomer feed composition was varied from run to run, it was found that high styrene contents tended to reduce the polymerization rate as well as the polymer molecular weight. Expected effects of styrene monomer feed composition on the polymer composition were also observed. No evidence of penultimate unit effects on composition was found. In addition, higher styrene feed contents yielded copolymers with more homogeneous composition distributions. This was most notably due to the proximity of the feed composition to the azeotropic composition.

ATR-FTIR spectrometry was shown to be a promising method to monitor monomer conversion and polymer composition for the styrene/butyl acrylate copolymer

system. However, results from ATR-FTIR spectrometry consistently underestimated the conversion compared with the traditional techniques. Despite the lack of interference of the monomers with toluene, it appeared that some interference between the two monomers affected some of the results. A variety of ATR-FTIR peaks were investigated for potential use as characteristic peaks but the results were in all cases less promising than 773.7 cm^{-1} for styrene monomer representing the C-H ring wag and 810 cm^{-1} for butyl acrylate monomer representing the $=CH_2$ twist.

7.2 Recommendations

From this thesis work, there are evident cases for improvement of the results. The following recommendations are made to that end:

Macromonomer/Acid system

1. In the residual monomer analysis, the composition of the residual monomer was obtained using GPC. The solubility of the macromonomers and the acid monomers was a key issue in this work. The results obtained from GPC were questionable due to the possible exclusion of the macromonomer in the injected sample during the sample filtration. In future work, if the polymer can also be dissolved and injected into the GPC, the confidence in the measured results would be greatly increase.
2. A key to the successful determination of reactivity ratios of this system is the ability to control the reaction rate in order to maintain low conversion levels or to at least generate a series of samples with varying conversion. The rate of

polymerization is greatly decreased if a solvent is used. Solution polymerization can help to lower the rate and obtain low conversion samples.

Styrene/Butyl Acylate system

1. In this work, the solvent effect has been determined only at 50wt.% toluene. In future work, an interesting investigation would be to extend the solvent effect study by varying the toluene concentration. The solvent effect could be determined for the whole range of toluene concentration in the feed.
2. Another interesting issue is to reproduce these experiments using other solvent than toluene. The results of those future experiments would determine the impact of other solvents on the reaction parameters. A good beginning should be to reproduce the Fernandez-Garcia, 1999 experiments with Styrene and Butyl Acrylate with benzene and benzonitrile as solvent.
3. The use of ATR-FTIR spectrometry was tested in this work for the conversion and composition determination. A goal to reach should be to follow the reaction kinetics using ATR-FTIR spectrometry, in order, to be able to get the same information obtained from the ^{1}H-NMR spectrometry. If successful, the expensive use of ^{1}H-NMR spectrometry analysis will not be necessary anymore.

Chapter 8

References

Arlman, E.J. and H.W. Melville, "Studies in Copolymerization. The Evaluation of the Kinetic Coefficients for the System Styrene - Butyl Acrylate", Proc. Roy. Soc. Lond. **A203**, 301-321, 1950.

Badeen, C., "Modeling Free-Radical Polymerizations with Depropagation using Java™: Methyl Methacrylate/a-methylstyrene at Elevated Temperatures", M.A.Sc. Thesis, University of Ottawa, Ottawa, Ontario, Canada, 2000.

Bradbury, J.H. and H.W. Melville, "The Co-polymerization of Styrene and Butyl Acrylate in Benzene Solution", Proc. Roy. Soc. Lond. **A222**, 456-470, 1954.

Brandrup, J., E.H. Immergut and E.A. Grulke, "Polymer Handbook, 4th Edition", Wiley Interscience, New York, Section 2, 181, 1999.

Brar, A.S. and C.V.V. Satyanarayana, "Microstructure Determination of Styrene - Butyl Acrylate Copolymer by NMR Spectroscopy", Polym. J., **24**, 9, 879-887, 1992.

Dubé, M.A., R. Amin Sanayei, A. Penlidis, P.M. Reilly and K.F. O'Driscoll, "A Microcomputer Program for Estimation of Copolymerization Reactivity Ratios", J. Polym. Sci.: Part A: Polym. Chem., **29**, 703-708, 1991.

Dubé, M.A., A. Penlidis and K.F. O'Driscoll, "A Kinetic Investigation of Styrene - Butyl Acrylate Copolymerization", Can. J. Chem. Eng., **68**, 974-987, 1990.

Dubé, M.A. and A. Penlidis, "A Systematic Approach to the Study of Multicomponent Polymerization Kinetics – The Butyl Acrylate/Methyl Methacrylate/Vinyl Acetate Example: 1. Bulk Copolymerization", Polymer, **36**, 587-598, 1995.

Dubé, M.A., J.B.P. Soares, A. Penlidis and A.E. Hamilec, "Mathematical Modeling of Multicomponent Chain-Growth Polymerizations in Batch. Semi-Batch, and Continuous Reactors: A Review", Ind. Eng. Chem. Res., **36**, 966-1015, 1997.

Fernandez-Garcia, M., M. Fernandez-Sanz, E.L. Madruga, R. Cuervo-Rodriguez, V. Hernandez-Gordo, M.C. Fernandez-Monreal, "Solvent effects on the Free-Radical Copolymerization of Styrene with Butyl Acrylate. I. Monomer Reactivity Ratios", J. Polym. Sci.: Part A: Polym. Chem., **38**, 60-67, 2000.

Gruber, E. and K.L. Knell, "Bestimmung der chemischen Heterogenistat Statistischer Copolymerer anhand von Untersuchungen an Poly(styrol-co-butylacrylat) und Poly(styrol-co-butylmethacrylat)", Makromol. Chem. **179**, 733-746, 1978.

Hamaide, T., A. Revillon and A. Guyot, "Réactivité de Macromères du Polyoxyéthylène en Copolymérisation Radicalaire", Eur. Polym. J., **20**, 9, 855-861, 1984.

Hua, H., M.A. Dubé, "In-line monitoring of emulsion homo- and copolymerizations using ATR-FTIR spectrometry", Polym. React. Eng., **10**, 21-40, 2002.

Hua, H., M.A. Dubé, "Off-line monitoring of butyl acrylate, methyl methacrylate and vinyl acetate homo- and copolymerizations in toluene using ATR-FTIR spectrometry", Polymer, **42**, 6009-6018, 2001.

Hua, H., M.A. Dubé, "Terpolymerization monitoring with ATR-FTIR spectrometry", J. Polym. Sci.: Part A: Polym. Chem., **39**, 11, 1860-1876, 2001.

Jeon, S.H. and T. Ree, "Characterization of Poly(carboxylic Acid)/Poly(ethylene Oxide) Blends Formed Through Hydrogen Bonding by Spectroscopic and Calorimetric Analyses", J. Polym. Sci.: Part A: Polym. Chem., **26**, 1419-1428, 1988.

Jovanovic, R. and M.A. Dubé, "Off-line monitoring of butyl acrylate and vinyl acetate homopolymerization and copolymerization in toluene", J. Appl. Polym. Sci., **82**, 12, 2958-2977, 2001.

Kelen, T., and F. Tudos, "Analysis of the Linear Methods for Determining Copolymerization Reactivity Ratios. I. A New Improved Linear Graphic Method", J. Macrom. Sci. and Chem.: Part A, **9**, 1, 1-27, 1975

Kostanski, L.K. and A.E. Hamielec, "Influence of Temperature on Butyl Acrylate - Styrene Copolymerization Parameters", Polymer, **23**, 17, 3706-3710, 1991.

Lahoud, N., "Reactivity Ratio Estimation for the Terpolymerization of Styrene/Butyl Acrylate/Methacrylic Acid", BSc. Thesis, University of Ottawa, Ottawa, Ontario, Canada, 1998.

Mayo, F.R. and F.M. Lewis, "Copolymerization. I. A basis for comparing behavior of Monomers in Copolymerization; The Copolymerization of Styrene and Methyl Methacrylate", J. Am. Chem. Soc., **66**, 1594-1601, 1944.

Meyer, V.E. and G.G. Lowry, "Integral and differential binary copolymerization equations", J. Polym. Sci.: Part A, **3**, 2843-2851, 1965.

O'Driscoll, K.F. and P.M. Reilly, "Determination of Reactivity Ratios in Copolymerization", Makromol. Chem., Macromol. Symp., **10-11**, 355-374, 1987.

Odian, G., "Principles of Polymerization", Third Edition, Wiley-Interscience, New York, 768, 1991.

Patino-Leal, H., P.M. Reilly and J. O'Driscoll, "On the Estimation of Reactivity Ratios", J. Polym. Sci. Letter Ed., **18**, 219-227, 1980.

Polic, A.L., T.A. Duever and A. Penlidis, "Case Studies and Literature Review on the Estimation of Copolymerization Reactivity Ratios", J. Polym. Sci.: Part A: Polym. Chem., **36**, 813-822, 1998.

Rossignoli, P.J. and T.A. Duever, "The Estimation of Copolymer Reactivity Ratios: A Review and Case Studies Using the Error-in-Variable Model and Nonlinear Least Squares", Polym. React. Eng. J., **3**, 4, 361-395, 1995.

Tidwell, P.W. and G.A. Mortimer, "An Improved Method of Calculating Copolymerization Reactivity Ratios", J. Polym. Sci.: Part A, **3**, 369-387, 1965.

Ziaee, F. and M. Nekoomanesh, "Monomer Reactivity Ratios of Styrene - Butyl Acrylate Copolymers at Low and High Conversion", Polymer, **39**, 1, 203-207, 1997.

Appendix A

Sty/BA Copolymerization Data, Reactivity Ratio Estimation

Appendix A:
Sty/BA Copolymerization Data, Reactivity Ratio Estimation

Table A.1: Recipes for the reactivity ratio estimation runs

	BC1 to BC4 SC1 to SC4 f_{Sty}=0.6768	BC5 to BC7 SC5 to SC7 f_{Sty}=0.0838
Mass of styrene in reaction mixture (g)	95.5611	10.9830
Mass of butyl acrylate in reaction mixture (g)	56.1510	147.7593
Total mass of monomers in reaction mixture (g)	151.7121	158.7423
Mass used for bulk copolymerization (g)	101.6639	105.8470
Mass of initiator added for bulk copolymerization (g)	0.3697	0.3798
Temperature	60°C	60°C
Mass used for solution copolymerization (g)	50.0482	52.8953
Mass of toluene added (g)	50.1400	52.9013
Mass of reaction mixture for solution copolymerization (g)	100.1882	105.7966
Mass of initiator added for solution copolymerization (g)	0.3857	0.4046
Temperature	60°C	60°C

Table A.2: Gravimetric Results, Bulk Runs

Ampoule Number	Empty Ampoule (g)	Reaction Mixture (g)	Glass Joint (g)	Weight Empty Dish (g)	Weight Dish + Polymer (g)	Conversion (wt.%)
BC1	64.0062	22.6643	6.4524	96.2448	97.9952	0.0772
BC2	64.2278	22.6309	7.0981	122.8415	124.0019	0.0513
BC3	58.9940	22.5669	6.0236	124.4057	125.6168	0.0537
BC4	60.3602	22.5468	5.2366	116.0455	117.2251	0.0523
BC5	61.2794	22.4373	5.6309	121.3724	122.0831	0.0317
BC6	61.3574	22.5843	5.7683	124.0216	124.9102	0.0393
BC7	59.2771	22.5864	6.4353	100.8581	101.5998	0.0328

Table A.3: Gravimetric Results, Solution Runs

Ampoule Number	Empty Ampoule (g)	Reaction Mixture (g)	Glass Joint (g)	Weight Empty Dish (g)	Weight Dish + Polymer (g)	Conversion (wt.%)
SC1	64.8594	22.1241	5.7977	100.1130	100.8027	0.0312
SC2	66.2092	22.1676	6.9442	97.4090	98.0881	0.0306
SC3	64.2052	22.1086	5.3281	117.9452	118.6437	0.0316
SC4	63.3069	22.2057	5.5827	96.2448	96.9346	0.0311
SC5	65.4991	22.2186	5.9368	86.6889	87.0631	0.0168
SC6	58.9178	21.8559	5.7339	120.7862	121.0651	0.0128
SC7	62.7258	22.0905	6.4308	93.5184	93.9621	0.0201

Table A.4: Composition Data For Bulk Sty/BA Reactivity Ratio Estimation

Ampoule Number	f_{Sty}	f_{BA}	Area under H_5 peak	Area under OCH_2 peak	F_{Sty}	F_{BA}
BC1	0.6768	0.3232	397.7	69.5	0.69595	0.30405
BC2	0.6768	0.3232	400.0	66.9	0.70516	0.29484
BC3	0.6768	0.3232	396.2	68.9	0.69698	0.30302
BC4	0.6768	0.3232	384.2	69.0	0.69014	0.30986
BC5	0.0838	0.9162	60.1	68.3	0.26034	0.73966
BC6	0.0838	0.9162	61.6	69.0	0.26314	0.73686
BC7	0.0838	0.9162	59.1	67.7	0.25881	0.74119

Table A.5: Composition Data For Solution Sty/BA Reactivity Ratio Estimation

Ampoule Number	f_{Sty}	f_{BA}	Area under H_5 peak	Area under OCH_2 peak	F_{Sty}	F_{BA}
SC1	0.3056	0.1459	398.3	64.7	0.71119	0.28881
SC2	0.3056	0.1459	396.5	65.7	0.70709	0.29291
SC3	0.3056	0.1459	411.0	66.2	0.71292	0.28708
SC4	0.3056	0.1459	405.9	65.1	0.71380	0.28620
SC5	0.0356	0.3867	63.2	69.4	0.26700	0.73300
SC6	0.0356	0.3867	65.9	69.8	0.27413	0.72587
SC7	0.0356	0.3867	61.6	67.4	0.26771	0.73229

Appendix B

Sty/BA Copolymerization Data, High Conversion Runs

Appendix B:
Sty/BA Copolymerization Data, High Conversion Runs

Table B.1: Recipes For High Conversion Runs

	20 wt.% Styrene (for 20HCxx)	40 wt.% Styrene (for 40HCxx)	60 wt.% Styrene (for 60HCxx)	80 wt.% Styrene (for 80HCxx)
Styrene (g)	10.0105	20.0107	30.0034	40.0193
Butyl Acrylate (g)	40.0387	30.0200	20.0029	10.0360
Toluene (g)	50.1116	50.0812	50.0381	50.1060
Initiator (g)	1.8787	1.8921	1.8627	1.8639
Chain Transfer (g)	0.5802	0.5787	0.5868	0.6438
Temperature	60°C	60°C	60°C	60°C

Table B.2: Gravimetric Results, High Conversion Runs (20 wt.% Sty)

Ampoule Number	Time (min.)	Filled Ampoule (g)	Broken Ampoule (g)	Reaction Mixture - Toluene (g)	Empty Dish (g)	Dish + Polymer (g)	Conversion (wt.%)
20HC01	40	12.6599	9.7494	1.4562	100.0180	10.1815	11.2282
20HC02	80	12.3325	9.6895	1.3223	124.2860	124.5571	20.5018
20HC03	120	12.8724	10.1019	1.3861	100.7651	101.1135	25.1350
20HC04	160	12.4411	9.7212	1.3608	86.5721	87.0338	33.9286
20HC05	200	12.4874	9.7340	1.3776	122.7243	123.2386	37.3342
20HC06	240	12.4496	9.7600	1.3456	123.9093	124.5381	46.7288
20HC06B	240	12.4068	9.9107	1.2488	116.2218	116.8261	48.3894
20HC07	280	12.4753	9.8380	1.3195	121.2370	121.9389	53.1955
20HC08	320	12.6839	9.8862	1.3997	96.8286	97.6241	56.8327
20HC09	360	12.6369	9.8708	1.3839	97.2878	98.1536	62.5618
20HC10	400	12.6891	9.9895	1.3506	115.9240	116.8541	68.8636
20HC11	440	12.4990	9.8745	1.3131	117.8124	118.7833	73.9414
20HC12	480	12.8148	10.1283	1.3441	120.6477	121.7480	81.8623
20HC13	520	12.2640	9.7623	1.2516	119.8785	120.9961	89.2916
20HC14	560	123492	9.5879	1.3815	115.9948	117.2093	87.9110
20HC15	600	12.5323	9.7380	1.3980	117.8026	119.0117	86.4866

Table B.3: Gravimetric Results, High Conversion Runs (40 wt.% Sty)

Ampoule Number	Time (min.)	Filled Ampoule (g)	Broken Ampoule (g)	Reaction Mixture - Toluene (g)	Weight Empty Dish (g)	Weight Dish + Polymer (g)	Conversion (wt.%)
40HC01	100	12.5160	9.8349	1.3412	100.0185	100.2927	20.4440
40HC02	200	12.8320	10.1510	1.3412	123.9306	124.3840	33.8061
40HC03	300	12.3524	9.6819	1.3359	100.7758	101.3733	44.7256
40HC04	400	12.9213	10.2088	1.3569	86.5895	87.3003	52.3828
40HC05	500	12.7591	10.0562	1.3521	122.7351	123.5862	62.9451
40HC06	600	12.7794	10.0410	1.3699	124.3014	125.2464	68.9836
40HC07	700	12.3664	9.7265	1.3206	121.2684	122.2473	74.1245
40HC08	800	12.1749	9.4757	1.3503	96.8461	97.9100	78.7910
40HC09	900	12.7955	8.5161	1.3579	97.2933	98.3945	81.0958
40HC10	1000	12.6534	9.8407	1.4071	115.9439	117.0922	81.6099
40HC11	1100	12.5049	9.7499	1.3782	117.8396	119.0449	87.4550
40HC12	1200	12.6652	9.8991	1.3837	120.6730	121.9225	90.2983

Table B.4: Gravimetric Results, High Conversion Runs (60 wt.% Sty)

Ampoule Number	Time (min.)	Filled Ampoule (g)	Broken Ampoule (g)	Reaction Mixture - Toluene (g)	Weight Empty Dish (g)	Weight Dish + Polymer (g)	Conversion (wt.%)
60HC01	120	12.4545	9.7775	1.389	99.9991	100.2964	22.2044
60HC02	240	12.5108	9.8226	1.3445	119.8816	120.3604	35.6110
60HC03	360	12.3272	9.6975	1.3153	115.9949	116.6604	50.5981
60HC04	480	12.2200	9.6694	1.2757	117.8024	118.6124	63.4943
60HC06	720	12.4054	9.6500	1.3781	115.8451	116.7909	68.6288
60HC07	840	12.4856	9.7824	1.3520	111.4414	112.4628	75.5457
60HC08	960	12.7119	9.9616	1.3756	93.4022	94.5178	81.0999
60HC09	1080	12.4668	9.7534	1.3571	96.1482	97.3379	87.6629
60HC10	1200	12.8963	10.1894	1.3539	115.9522	117.1932	91.6625
60HC11	1320	12.4993	9.8115	1.3443	117.8449	119.1812	99.4029
60HC12	1440	12.7959	10.1042	1.3463	120.6797	122.0125	98.9989

Table B.5: Gravimetric Results, High Conversion Runs (80 wt.% Sty)

Ampoule Number	Time (min.)	Filled Ampoule (g)	Broken Ampoule (g)	Reaction Mixture - Toluene (g)	Weight Empty Dish (g)	Weight Dish + Polymer (g)	Conversion (wt.%)
80HC01	120	12.7874	9.9878	1.4005	80.9448	81.2279	20.2141
80HC02	240	12.6958	9.8915	1.4029	91.2930	91.7802	34.7291
80HC03	360	12.9207	10.1530	1.3846	81.6148	82.2556	46.2822
80HC04	480	12.3389	9.5876	1.3763	86.3963	87.1711	56.2940
80HC05	600	12.4244	9.6931	1.3663	123.9344	124.7783	61.7635
80HC06	720	12.4282	9.6240	1.4028	121.2857	122.2277	67.1509
80HC07	840	13.1890	10.3687	1.4109	97.2917	98.3526	75.1951
80HC08	960	12.6039	9.7626	1.4214	122.7495	123.8691	78.7691
80HC09	1080	12.6355	9.7987	1.4191	100.7627	101.9132	81.0715
80HC10	1200	12.6555	9.8919	1.3825	96.8521	98.0374	85.7360
80HC11	1320	12.3480	9.5693	1.3901	124.3099	125.5748	90.9965
80HC12	1440	12.5623	9.7485	1.4076	86.5974	87.9029	92.7457

Table B.6: Composition Data For Sty/BA High Conversion Runs (20 Wt.% Sty)

Ampoule Number	f_{Sty}	f_{BA}	Area under H_5 peak	Area under OCH_2 peak	F_{Sty}	F_{BA}
20HC01	0.2353	0.7647	123.6	61.3	0.44645	0.55355
20HC04	0.2353	0.7647	116.4	65.8	0.41438	0.58562
20HC07	0.2353	0.7647	100.3	66.9	0.37488	0.62512
20HC10	0.2353	0.7647	83.5	65.9	0.33635	0.66365
20HC12	0.2353	0.7647	69.4	66.2	0.29544	0.70456
20HC14	0.2353	0.7647	56.9	65.3	0.25846	0.74154

Table B.7: Composition Data For Sty/BA High Conversion Runs (40 Wt.% Sty)

Ampoule Number	f_{Sty}	f_{BA}	Area under H_5 peak	Area under OCH_2 peak	F_{Sty}	F_{BA}
40HC01	0.4506	0.5494	210.9	60.4	0.58276	0.41724
40HC03	0.4506	0.5494	207.2	64.2	0.56350	0.43650
40HC05	0.4506	0.5494	196.2	63.7	0.55198	0.44802
40HC07	0.4506	0.5494	186.7	63.8	0.53928	0.46072
40HC09	0.4506	0.5494	173.6	64.7	0.51767	0.48233
40HC12	0.4506	0.5494	162.4	63.7	0.50490	0.49510

Table B.8: Composition Data For Sty/BA High Conversion Runs (60 wt.% Sty)

Ampoule Number	f_{Sty}	f_{BA}	Area under H_5 peak	Area under OCH_2 peak	F_{Sty}	F_{BA}
60HC01	0.6486	0.3514	348.6	57.5	0.70803	0.29197
60HC03	0.6486	0.3514	351.1	63.9	0.68729	0.31271
60HC06	0.6486	0.3514	347.4	62.4	0.69011	0.30989
60HC08	0.6486	0.3514	349.4	61.5	0.69443	0.30557
60HC10	0.6486	0.3514	348.1	60.5	0.69711	0.30289
60HC12	0.6486	0.3514	346.2	62.5	0.68902	0.31098

Table B.9: Composition Data For Sty/BA High Conversion Runs (80 wt.% Sty)

Ampoule Number	f_{Sty}	f_{BA}	Area under H_5 peak	Area under OCH_2 peak	F_{Sty}	F_{BA}
80HC01	0.8307	0.1693	608.0	46.0	0.84094	0.15906
80HC03	0.8307	0.1693	634.5	47.8	0.84151	0.15849
80HC05	0.8307	0.1693	703.0	54.9	0.83666	0.16334
80HC07	0.8307	0.1693	742.9	53.6	0.84719	0.15281
80HC10	0.8307	0.1693	783.7	58.6	0.84251	0.15749
80HC12	0.8307	0.1693	790.3	57.3	0.84655	0.15345

Table B.10: Gel Permeation Chromatography (GPC) Results

	Ampoule Number	Mn	Mw	Polydispersity Index
20 wt.% Sty	20HC01	5236	7820	1.49
	20HC04	7435	13307	1.79
	20HC07	9110	19037	2.09
	20HC10	10474	23631	2.26
	20HC12	11119	26985	2.43
	20HC14	11438	28279	2.47
40 wt.% Sty	40HC01	5652	8982	1.59
	40HC03	8327	16797	2.02
	40HC05	9505	20085	2.11
	40HC07	10133	21002	2.07
	40HC09	10266	21427	2.09
	40HC12	10308	21384	2.07
60 wt.% Sty	60HC01	5484	8695	1.59
	60HC03	8352	17210	2.06
	60HC06	10103	21374	2.12
	60HC08	10420	21799	2.09
	60HC10	9893	19812	2.00
	60HC12	9814	19561	1.99
80 wt.% Sty	80HC01	4927	7559	1.53
	80HC03	8021	16135	2.01
	80HC05	9011	18116	2.01
	80HC07	9397	18684	1.99
	80HC10	10217	19309	1.89
	80HC12	9417	18494	1.96

Table B.11: ATR-FTIR Spectrometry Results (20 wt.% Sty)

Ampoule Number	Peak Height at 778 cm^{-1}	Styrene Conversion (wt.%)	Peak Height at 814 cm^{-1}	Butyl Acrylate Conversion (wt.%)	Overall Conversion (wt.%)
Raw Mix	0.1362		0.3437		
20HC01	0.1264	7.1953	0.3392	1.3093	2.4835
20HC02	0.1092	19.8238	0.3224	6.1973	8.9116
20HC03	0.0949	30.3231	0.3084	10.2706	14.2636
20HC04	0.0816	40.0881	0.2937	14.5476	19.6315
20HC05	0.0694	49.0455	0.2789	18.8537	24.8614
20HC06	0.0564	58.5903	0.2602	24.2944	31.1153
20HC06B	0.0514	62.2614	0.2444	28.8915	35.5216
20HC07	0.0463	66.0059	0.2415	29.7352	36.9438
20HC08	0.0388	71.5125	0.2248	34.5941	41.9260
20HC09	0.0302	77.8267	0.2044	40.5295	47.9297
20HC10	0.0242	82.2320	0.1818	47.1050	54.0635
20HC11	0.0188	86.1968	0.1545	55.0480	61.2019
20HC12	0.0138	89.8678	0.1240	63.9220	69.0255
20HC13	0.0097	92.8781	0.0739	78.4987	81.2734
20HC14	0.0083	93.9060	0.0472	86.2671	87.6857
20HC15	0.0074	94.5668	0.0309	91.0096	91.6069

Table B.12: ATR-FTIR Spectrometry Results (40 wt.% Sty)

Ampoule Number	Peak Height at 778 cm^{-1}	Styrene Conversion (wt.%)	Peak Height at 814 cm^{-1}	Butyl Acrylate Conversion (wt.%)	Overall Conversion (wt.%)
Raw Mix	0.2445		0.2748		
40HC01	0.2032	16.8916	0.2451	10.8079	13.2278
40HC02	0.1692	30.7975	0.2216	9.3661	17.9199
40HC03	0.1386	43.3129	0.1976	19.1820	28.8045
40HC04	0.1192	51.2474	0.1827	25.2761	35.6278
40HC05	0.0943	61.4315	0.1611	34.1104	44.9926
40HC06	0.0769	68.5481	0.1424	41.7587	52.4207
40HC07	0.0630	74.2331	0.1252	48.7935	58.9091
40HC08	0.0343	85.9714	0.0732	70.0613	76.3478
40HC09	0.0436	82.1677	0.0978	60.0000	68.7969
40HC10	0.0372	84.7853	0.0859	64.8671	72.7603
40HC11	0.0326	86.6667	0.0752	69.2434	76.1353
40HC12	0.0292	88.0573	0.0664	72.8425	78.8484

Table B.13: ATR-FTIR Spectrometry Results (60 wt.% Sty)

Ampoule Number	Peak Height at 778 cm^{-1}	Styrene Conversion (wt.%)	Peak Height at 814 cm^{-1}	Butyl Acrylate Conversion (wt.%)	Overall Conversion (wt.%)
Raw Mix	0.3385		0.1837		
60HC01	0.2945	12.9985	0.1632	11.1595	12.2551
60HC02	0.2570	24.0768	0.1441	21.5569	23.0542
60HC03	0.2221	34.3870	0.1302	29.1236	32.2611
60HC04	0.1896	43.9882	0.1219	33.6418	39.8242
60HC06	0.1579	53.3530	0.0928	49.4829	51.7720
60HC07	0.1407	58.4343	0.0828	54.9265	56.9949
60HC08	0.1192	64.7858	0.0621	66.1949	65.3079
60HC09	0.0997	70.5465	0.0568	69.0800	69.9155
60HC10	0.0875	74.1507	0.0478	73.9793	74.0350
60HC11	0.0816	75.8936	0.0438	76.1568	75.9506
60HC12	0.0747	77.9321	0.0380	79.3141	78.4350

Table B.14: ATR-FTIR Spectrometry Results (80 wt.% Sty)

Ampoule Number	Peak Height at 778 cm^{-1}	Styrene Conversion (wt.%)	Peak Height at 814 cm^{-1}	Butyl Acrylate Conversion (wt.%)	Overall Conversion (wt.%)
Raw Mix	0.4438		0.0923		
80HC01	0.3396	23.4790	0.0810	12.2427	21.2047
80HC02	0.3600	18.8824	0.0701	24.0520	19.8987
80HC03	0.3228	27.2645	0.0615	33.3694	28.4597
80HC04	0.2898	34.7003	0.0570	38.2449	35.3752
80HC05	0.2581	41.8432	0.0434	52.9794	44.0314
80HC06	0.2315	47.8369	0.0381	58.7216	49.9686
80HC07	0.2118	52.2758	0.0303	67.1723	55.2066
80HC08	0.1941	56.2641	0.0257	72.1560	59.3902
80HC09	0.1751	60.5453	0.0215	76.7064	63.7210
80HC10	0.1629	63.2943	0.0183	80.1733	66.6110
80HC11	0.1485	66.5390	0.0151	83.6403	69.8970
80HC12	0.1377	68.9725	0.0128	86.1322	72.3397

Appendix C

Sty/BA High Conversion GPC Data

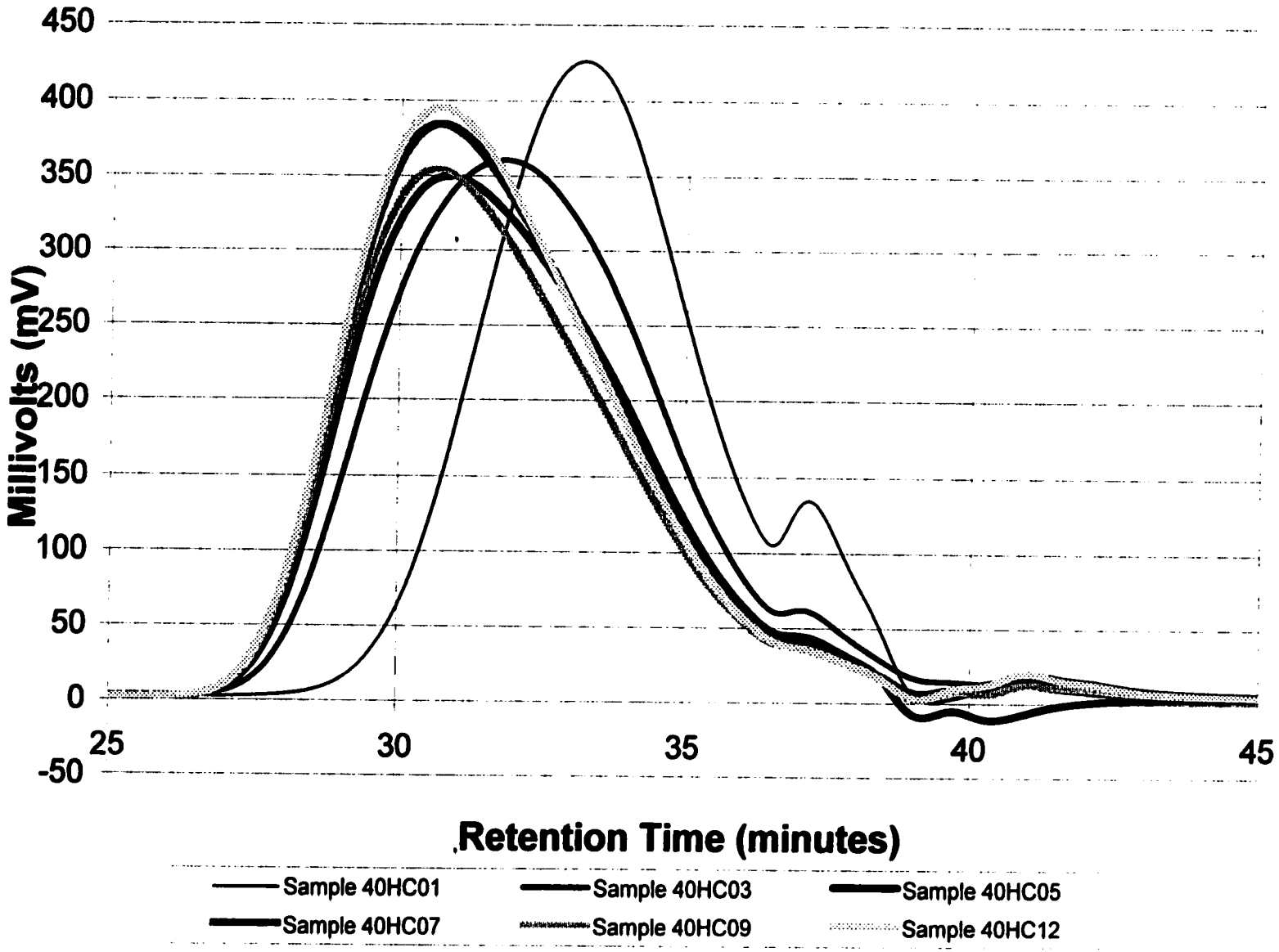

Figure C.1: GPC Curves for high conversion runs at 40 wt.% Styrene

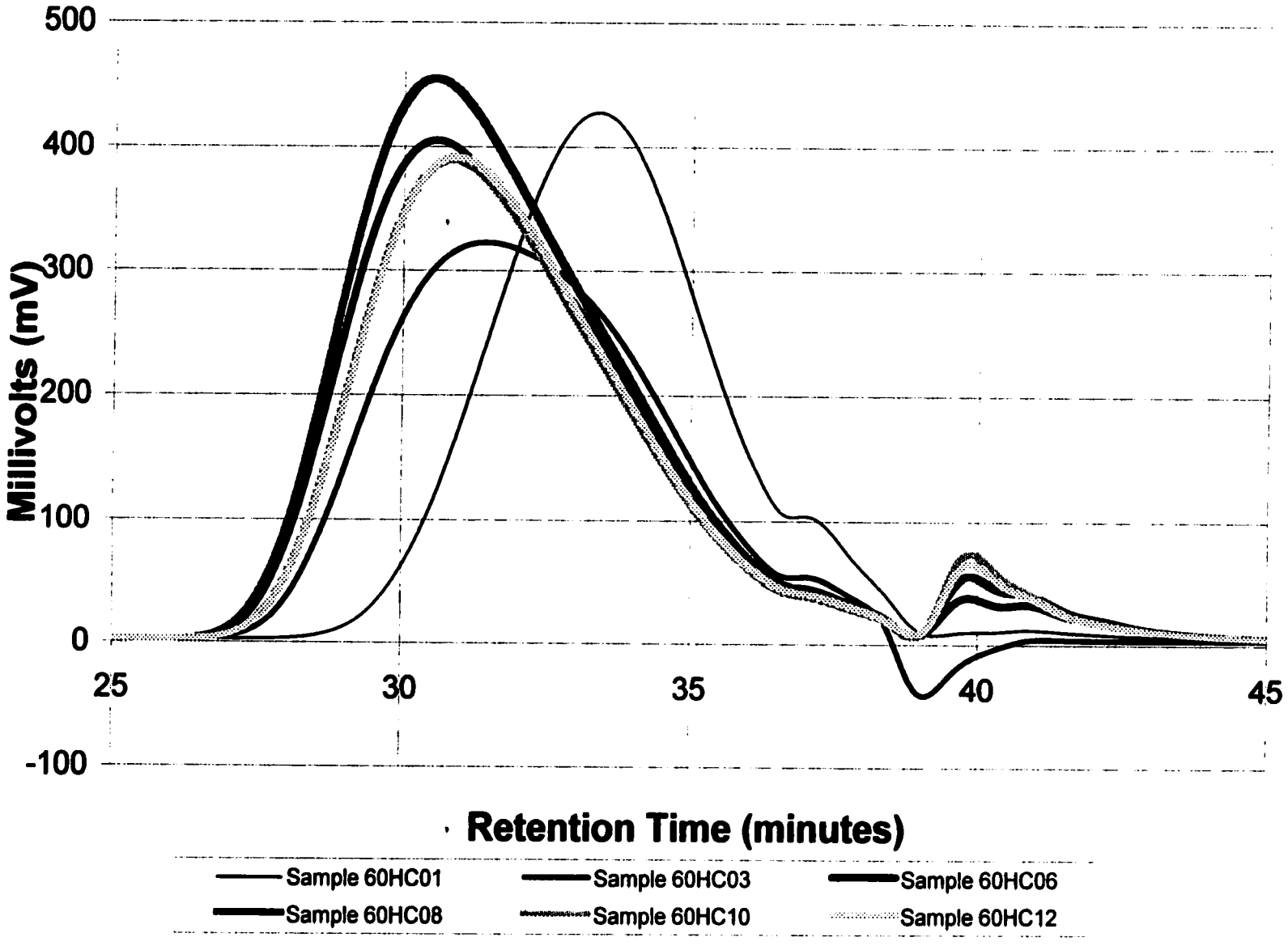

Figure C.2: GPC Curves for high conversion runs at 60 wt.% Styrene

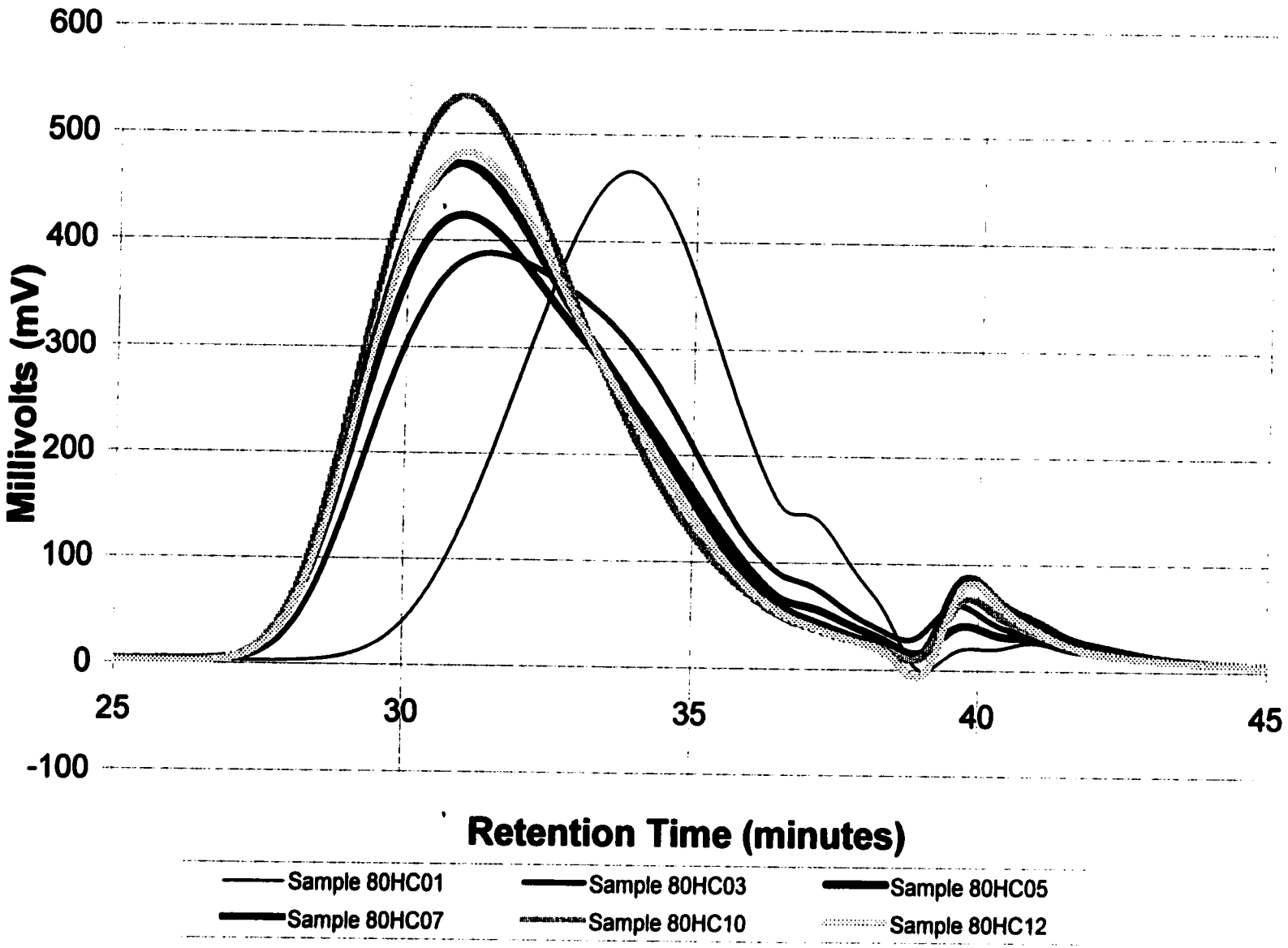

Figure C.3: GPC Curves for high conversion runs at 80 wt.% Styrene

Appendix D

Sample Calculations

Appendix D:
Sample Calculations

High conversion solution polymerization run from Ampoule Number 80HC01 (80 wt.% Sty)

Let 1 denote Styrene and 2 denote Butyl Acrylate

D.1 Reaction Recipe

Monomer feed: $m_1 = 40.0193$ g and $m_2 = 10.0360$ g
Solvent used: $m_{Toluene} = 50.1060$ g
Other Ingredients: $m_{AIBN} = 1.8639$ g and $m_{CTA} = 0.6438$ g
Total mass: 102.6690 g
In solution polymerization, total mass (neglecting solids): 100.1613 g

Monomer mole fraction f_1: $f_1 = \dfrac{\frac{m_1}{MW_1}}{\frac{m_1}{MW_1}+\frac{m_2}{MW_2}}$ identically f_2: $f_2 = \dfrac{\frac{m_2}{MW_2}}{\frac{m_1}{MW_1}+\frac{m_2}{MW_2}}$

where $MW_1 = 104.1512$ g/mol and $MW_2 = 128.1706$ g/mol
After the calculations: $f_1 = 0.8307$ and $f_2 = 0.1693$

Monomer moles n_1: $n_1 = \dfrac{m_1}{MW_1}$ and also $n_2 = \dfrac{m_2}{MW_2}$

We obtain from those relations: $n_1 = 0.3842$ moles and $n_2 = 0.0783$ moles

Monomer weight fraction w_1: $w_1 = \dfrac{m_1 + m_2}{Total \cdot mass} = 0.4997$

Solvent weight fraction $w_{Toluene} = \dfrac{m_{Toluene}}{Total \cdot mass} = 0.5003$

D.2 Monomer Conversion and Polymer Composition Calculation by Gravimetry and ^{1}H-NMR Spectrometry Methods

At Reaction Time: t = 120 minutes

Overall Conversion X (wt%)

$$X(wt\%) = \frac{Weight \cdot dried \cdot sample \cdot and \cdot dish - Weight \cdot empty \cdot dish}{w_{Toluene} * (Weight \cdot dish \cdot and \cdot sample - Weight \cdot empty \cdot dish)} = \frac{81.2279 - 80.9448}{0.5003 * (83.7444 - 80.9448)}$$

X (wt%) = 0.2021 = 20.21%

The copolymer composition and individual monomer conversions using ^{1}H-NMR spectrometry data (peak integration): $S_1 = 608.0$ and $S_2 = 46.0$

Copolymer Composition F_1 and F_2

$$F_1 = \frac{S_1/5}{S_1/5 + S_2/2} = 0.8409$$

$$F_2 = \frac{S_2/2}{S_1/5 + S_2/2} = 0.1591$$

Individual Monomer Conversion x_1^* and x_2^*

$$x_1^* = \frac{\frac{(MW_1 * f_1) + (MW_2 * f_2)}{(MW_1 * F_1) + (MW_2 * F_2)} * X * F_1}{f_1}$$

$$x_1^* = \frac{\frac{(104.1512 * 0.8307) + (128.1706 * 0.1693)}{(104.1512 * 0.8409) + (128.1706 * 0.1591)} * 0.2021 * 0.8409}{0.8307}$$

$$x_1^* = 0.205$$

Similarly, $x_2^* = 0.190$

D.3 Monomer conversion and polymer composition calculation by ATR-FTIR spectroscopy methods

At reaction time t = 0 minutes

$(Peak\ Height)_1 = 0.4438$ and $(Peak\ Height)_2 = 0.0923$

At reaction time t = 120 minutes

$(Peak\ Height)_1 = 0.3396$ and $(Peak\ Height)_2 = 0.0810$

1. Individual Monomer Conversion and Copolymer Composition

Individual Monomer Conversion

$$x_1^* = 1 - \frac{(Peak \cdot Height)_1\, at \cdot time \cdot t = 120}{(Peak \cdot Height)_1\, at \cdot time \cdot t = 0} = 1 - \frac{0.3396}{0.4438} = 0.2348$$

Similarly, $x_2^* = 0.1224$

Copolymer Composition F_1 and F_2

$$F_1 = \frac{(n_1 * x_1)}{(n_1 * x_1) + (n_2 * x_2)} = \frac{(0.3842 * 0.2348)}{(0.3842 * 0.2348) + (0.0783 * 0.1224)} = 0.9040$$

Similarly, $F_2 = 0.0960$

2. Overall Conversion

$$X(wt\%) = \left[\frac{w_1}{w_1 + w_2} * x_1\right] + \left[\frac{w_2}{w_1 + w_2} * x_2\right] = 0.1786$$

D.4 Azeotropic composition calculation

Using the reactivity ratios results from this study for solution polymerization

$$r_1 = 0.7966 \text{ and } r_2 = 0.1744$$

The determination of the aseotropic composition is given by the following relation:

$$f_{AZEO} = \frac{1-r_2}{2-r_1-r_2} = \frac{1-0.1744}{2-0.7966-0.1744} = 0.8023$$